DCs. To monitor the intracellular distribution of the liposomes, the encapsulated OVA and the liposome membrane were labeled, respectively, using FITC and Rh-PE. The labeled liposomes encapsulating FITC-OVA were added to DC2.4 cells and incubated for 4 h. Then, the cells were washed with buffer and observed using CLSM (Fig. 4). When DC2.4 cells were treated with the unmodified liposomes, punctate fluorescence of FITC-OVA was observed in the cells. In addition, fluorescence of Rh was observed at the same places that FITC-OVA fluorescence appeared. This result suggests that OVA molecules loaded in the unmodified liposomes were still trapped in the endosomes and/or the lysosomes. For cells treated with the SucPG liposomes, the fluorescence of FITC-OVA was also mostly punctate and overlapped with Rh-PE fluorescence. In contrast, for cells treated with MGluPG liposomes, diffuse fluorescence of FITC-OVA was observed in the cells, while fluorescence of Rh-PE remained punctate, indicating that the labeled OVA molecules were transferred into cytosol from endosome, where liposomal membrane remained trapped. Probably, the highly fusogenic MGluPG liposomes generate strong fusion ability in the weakly acidic environments of endosome and fuse with endosomal membrane, resulting in the release of entrapped OVA molecules into cytosol [9,10]. The SucPG liposomes only slightly induced the transfer of OVA into cytosol.

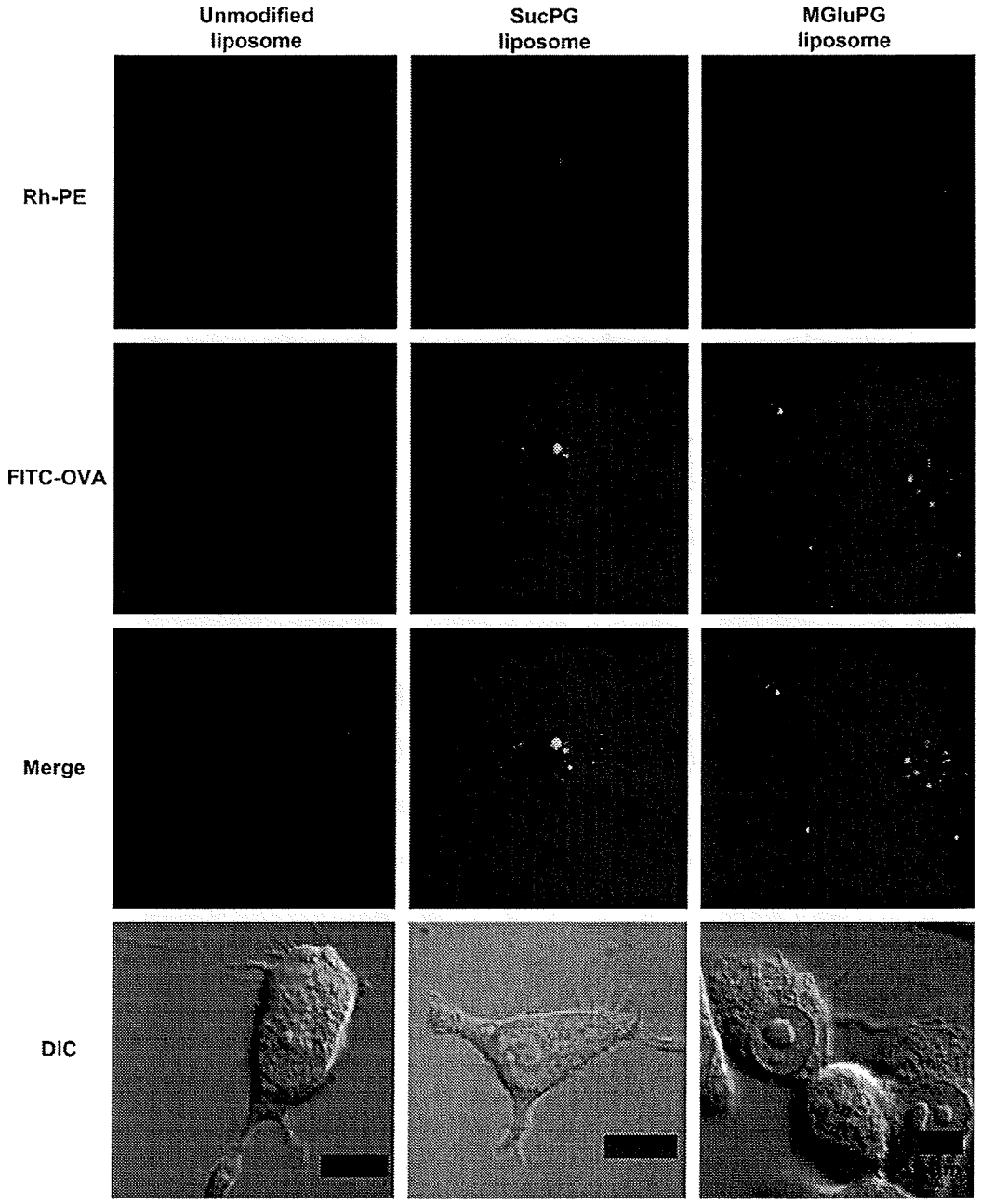

Fig. 4. CLSM images of DC2.4 cells treated with various liposomes labeled with Rh-PE and loaded with FITC-OVA. Liposomes prepared by extrusion method were used. DC2.4 cells were incubated with liposomes at 37 °C for 4 h in the serum-free medium, washed with HBSS and observed with CLSM. Scale bar represents 10 μm. Concentration of liposomal lipids for cellular treatment was 0.1 mM.

Therefore, it is implied that their fusion ability is insufficient to induce fusion or destabilization of endosomal membrane for efficient transfer of OVA molecules into cytosol (Fig. 2).

3.5. Induction of cellular immune responses

We examined the ability of these polymer-modified liposomes to activate cellular immunity. Although immunization is generally conducted *via* subcutaneous injection of antigen, we exploited the administration of antigen through nasal mucosa because antigen administration can be achieved using a noninvasive, needleless method in this immunization. It can also induce both mucosal and systemic immunities [11–13].

For this study, the C57BL/6 mice were immunized nasally twice with OVA-loaded liposomes containing MPL in the membrane as an adjuvant. One week later, splenocytes were collected from the immunized mice and stimulated with mitomycin C-treated E.G7-OVA cells. Then their toxicity toward E.G7-OVA cells, which are OVA-presenting recombinant cells derived from EL4 cells, was measured to estimate the induction of OVA-specific CTLs.

Fig. 5a shows cellular toxicities of the stimulated splenocytes recovered from mice that had been immunized with various OVA-loaded liposomes or free OVA. When free OVA was used for the immunization, CTL activity was almost identical to that of the case of untreated mice, indicating that free OVA has no ability to induce cellular immunity under experimental conditions. In addition, administration of the OVA-loaded unmodified liposomes increased

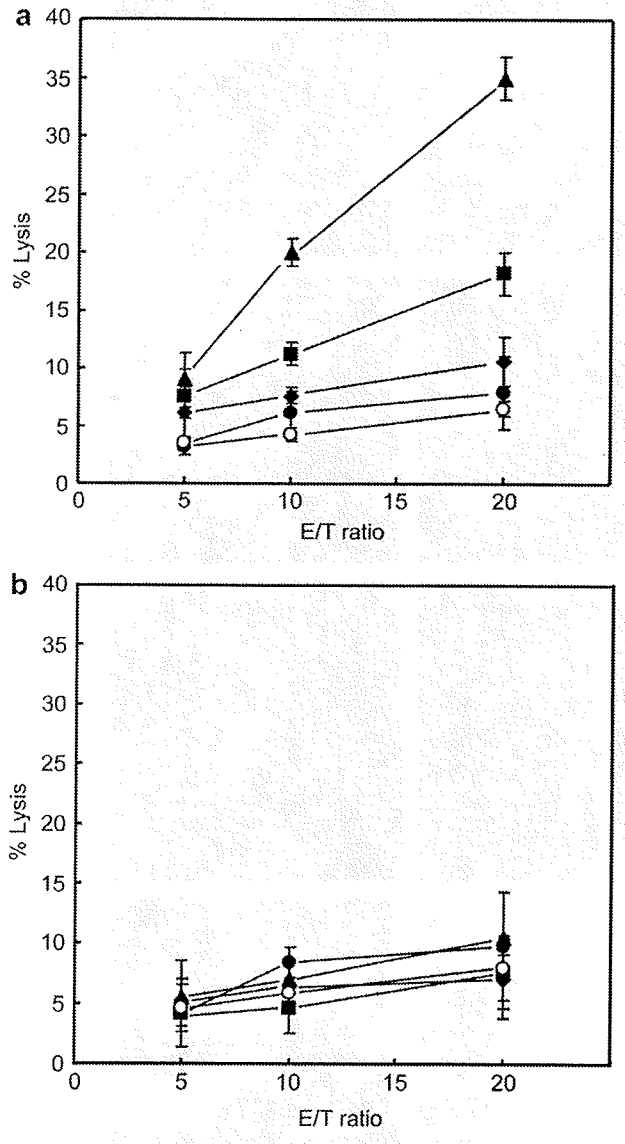

Fig. 5. OVA-specific cytotoxic T cell responses in spleen at Day 21 after nasal immunization with OVA solution (●), polymer-unmodified liposomes (◆), SucPG liposomes (■) and MGluPG liposomes (▲). Liposomes prepared by vortex method were used. Cytotoxic activity was measured by a LDH assay at indicated E/T ratios. E.G7-OVA cells (a) and EL4 cells (b) were used as target cells. T cell responses from mice without treatment (○) were also shown as a negative control.

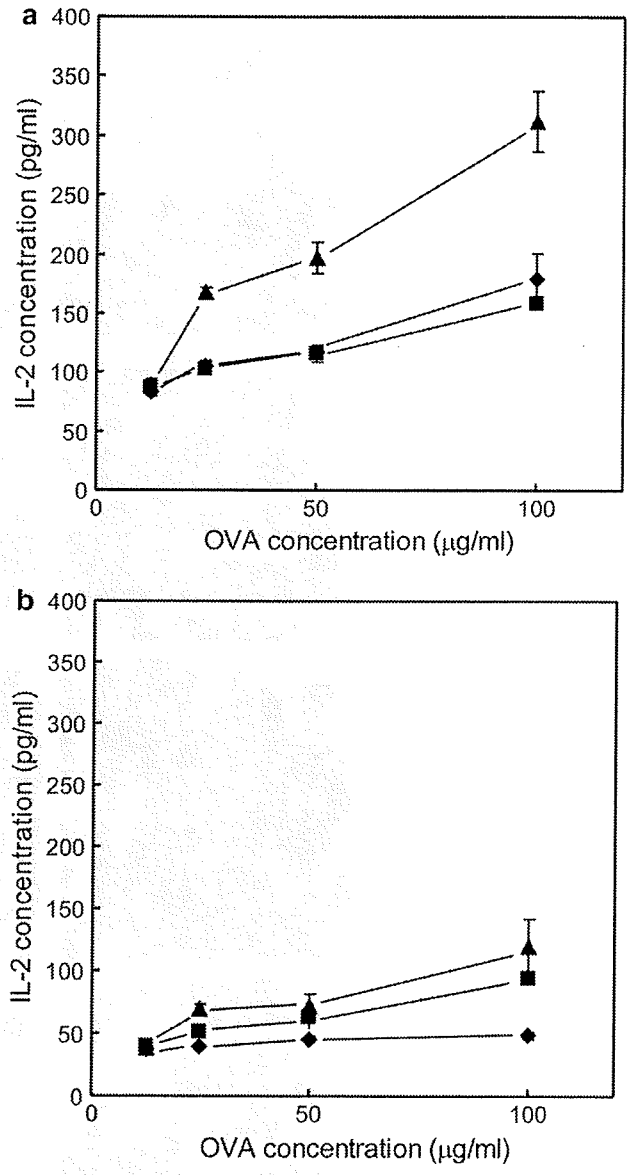

Fig. 6. Presentation of OVA-derived epitope peptides *via* MHC molecules in BMDCs. BMDCs were incubated with free OVA (diamonds), and OVA-loaded MGluPG-modified (triangles) and unmodified (squares) liposomes at varying OVA concentrations for 3 h. Liposomes prepared by extrusion method were used. Concentrations of IL-2 in the medium after co-culture of OVA-treated BMDCs with (a) CD8-OVA1.3 (specific for $OVA_{257-264}$/H-2 K^b complex) and (b) OT4H.1D5 (specific for $OVA_{265-277}$/I-A^b complex) cells for 24 h as a function of OVA concentration during the BMDCs treatment were shown. Each point represents means ± SD.

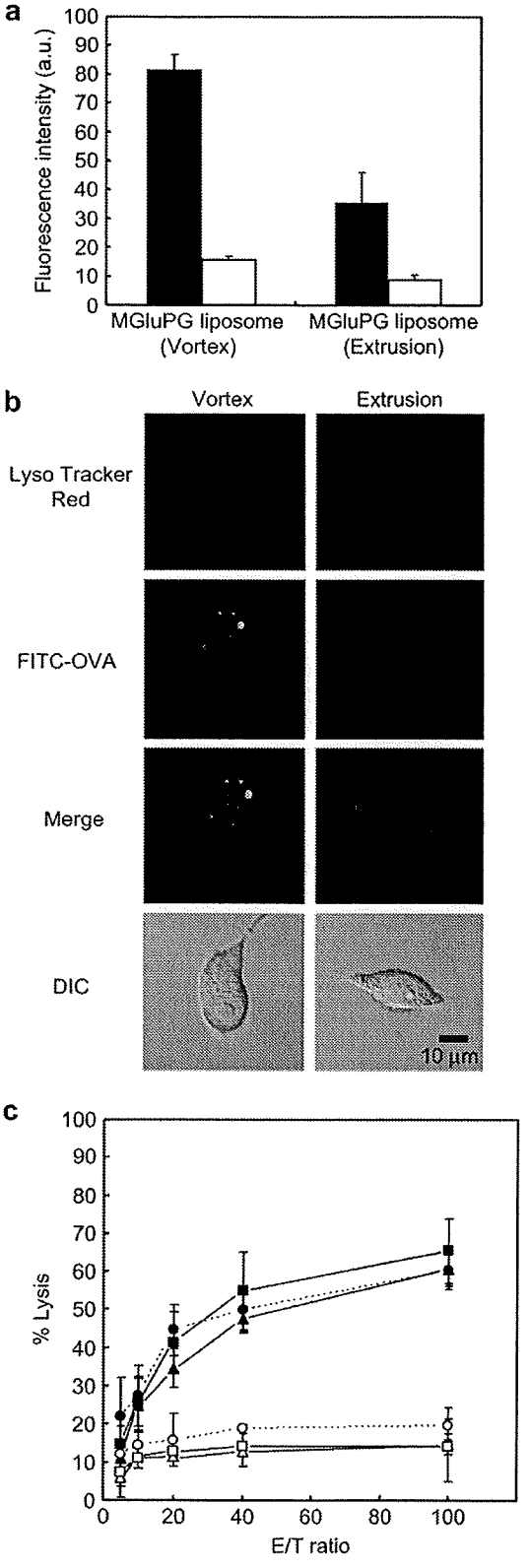

Fig. 7. (a) Effect of liposome size on delivery of FITC-OVA by MGluPG liposomes. DC2.4 cells were treated with FITC-OVA-loaded liposomes prepared by extrusion or vortex method in the serum-free medium at 4 °C (open) and 37 °C (closed) for 4 h, and then cellular association of FITC-OVA was estimated using flow cytometry. Each point is the mean ± SD ($n = 3$). OVA concentration was 50 μg/ml. (b) CLSM images of DC2.4 cells treated with FITC-OVA-loaded liposomes prepared by vortex method or extrusion method. DC2.4 cells were incubated with MGluPG-modified liposomes encapsulating FITC-OVA (50 μg of OVA/ml) in the serum-free medium at 37 °C for 4 h. (c) Effect of liposome size on OVA-specific cytotoxic T cell response. Mice were nasally immunized with OVA-loaded MGluPG liposome prepared by vortex method (triangles) or by extrusion method (squares). Mice were also immunized with CFA/OVA emulsion subcutaneously (circles). Cytotoxic activity of splenocytes of the immunized mice was measured by a LDH assay at indicated E/T ratios. E.G7-OVA cells (closed symbols) and EL4 cells (open symbols) were used as target cells.

the CTL activity only slightly. In contrast, when the polymer-modified liposomes containing OVA were used for immunization, higher CTL activities were observed. Especially, MGluPG-modified liposomes more efficiently induced activation of CTLs than the SucPG-modified liposomes did. Indeed, the same stimulated splenocytes did not exhibit cellular toxicity toward EL4 cells (Fig. 5b). Therefore, immunization with these polymer-modified liposomes containing OVA induced activation of OVA-specific CTLs. Considering that these polymer-modified liposomes showed a similar degree of cellular association with DCs (Fig. 3), it is likely that the difference in fusion ability between these liposomes caused their different abilities for cellular immune activation.

3.6. Estimation of antigen presentation

The highly fusogenic MGluPG-modified liposomes induced cellular immune response efficiently. Because the cellular immunity is activated through antigen presentation on the MHC class I molecules of antigen presenting cells (APCs), such as DCs, we expected that the liposome-mediated delivery of OVA molecules into cytosol of APCs caused the antigen presentation on the MHC class I molecules, engendering activation of cellular immunity. To confirm this mechanism, we further examined whether the MGluPG-modified liposomes actually possess the capability of inducing antigen presentation on the MHC class I on DCs.

The OVA-loaded liposomes or free OVA were added to BMDCs; then BMDCs were co-cultured with CD8-OVA1.3 or OT4H.1D5 cells, which respectively recognize MHC class I/peptide complexes or MHC class II/peptide complexes. Subsequently, MHC class-restricted antigen presentation was evaluated by detection of IL-2 secretion in supernatants of the co-cultured medium. Fig. 6 shows IL-2 production levels of the co-cultured medium of BMDCs treated with the OVA-loaded liposomes and free OVA. As depicted in Fig. 6a, interaction with BMDCs and OVA-loaded MGluPG-modified liposomes strongly enhanced IL-2 release from CD8-OVA1.3 cells. The BMDCs treated with either OVA-loaded in the plain liposomes or free OVA also promoted IL-2 release from the CD8-OVA1.3 cells, but the promotion occurred to a much lesser degree than the case of the OVA-loaded MGluPG-modified liposomes. This result suggests that the OVA-loaded MGluPG-modified liposomes induced antigen presentation through the MHC class I molecules on BMDCs more efficiently than free or plain liposome-encapsulated OVA. In contrast, BMDCs treated with these OVA-loaded liposomes or free OVA enhanced IL-2 release from OT4H.1D5 cells only slightly, suggesting that the OVA-loaded MGluPG-modified liposomes have no ability to induce MHC class II-mediated antigen presentation. These results demonstrate that the MGluPG-modified liposomes can induce antigen presentation through MHC class I molecules.

3.7. Influence of liposome size on cellular immunity activation

Finally, we examined the influence of liposome size on their ability to activate cellular immunity. First, MGluPG liposomes with diameters around 500 nm and 110 nm were prepared, respectively, using vortex and extrusion methods (Table 1). We compared the

respective efficiencies of the intracellular OVA delivery of these liposomes with different sizes. The amounts of encapsulated OVA per 1 nmol of liposomal lipid were estimated to be 0.77 μg for the large liposomes and 0.2 μg for the small liposomes. When the same amount of FITC-OVA was added to DC2.4 cells as encapsulated in the liposomes, approximately double the amount of FITC-OVA was taken up by the cells using the large liposomes than those using the small liposomes (Fig. 7a).

We also examined the intracellular distribution of OVA molecules delivered by these MGluPG liposomes of different sizes. The DC2.4 cells were incubated with these MGluPG liposomes encapsulating FITC-OVA for 4 h and then observed using CLSM (Fig. 7b). Strong and punctate fluorescence of FITC-OVA was observed in cells treated with large MGluPG liposomes. Punctate fluorescence of FITC-OVA is mostly overlapped with fluorescence of LysoTracker Red. Therefore, most FITC-OVA molecules remained trapped in the endosomes and lysosomes. The punctate fluorescence of FITC-OVA was still observed in the liposome-treated cells even after 24 h-incubation, indicating that FITC-OVA molecules were retained in endosome and lysosome for 24 h (data not shown). In contrast, cells treated with the small MGluPG liposomes displayed diffuse fluorescence of FITC-OVA, suggesting that these small liposomes delivered the antigenic protein efficiently into the cytosol.

The large MGluPG liposomes prepared by vortex showed less endosomal escape, compared to the small extruded MGluPG liposomes, although these liposomes were modified with the same fusogenic polymer MGluPG. Because the large liposome should have a multilamellar structure, only the outermost layer of the bilayer membranes with low curvature might contact with the target membrane, resulting in low efficiency of fusion. In fact, we evaluated fusion ability of the large MGluPG liposome by the same method used for evaluation of the small MGluPG liposome fusion (Fig. 2) and observed only 10% increase in R value after 3.5 h incubation at pH4.0, indicating a low fusion ability of the large MGluPG liposome (data not shown).

These liposomes encapsulating OVA were administered nasally; then CTL responses were evaluated as described above (Fig. 7c). Splenocytes of the immunized mice exhibited high toxicity toward OVA-presenting E.G7-OVA cells but almost no toxicity toward their parent EL4 cells, indicating that both liposomes were able to induce OVA-specific CTLs, irrespective of their size difference. Moreover, the CTLs derived with these OVA-loaded liposomes showed an almost identical level of toxicity to E.G7-OVA cells within the error bars. The large MGluPG liposomes delivered more OVA molecules to cells than the small liposomes. However, the latter introduced OVA molecules into the cytosol more efficiently than the former. Consequently, these liposomes might achieve CTL activation to a similar degree.

To evaluate the potential of MGluPG liposomes as an adjuvant, we compared their induced CTLs activity with that of CFA, which is widely used for induction of immune responses [26]. The result is also presented in Fig. 7c. Apparently, CTL activity induced by CFA is of a comparable level to that of MGluPG liposomes.

4. Conclusions

For this study, by modification of liposomes with carboxylated poly(glycidol) derivatives, such as SucPG and MGluPG, we prepared pH-sensitive fusogenic liposomes that can deliver antigenic proteins into the cytosol of DCs. We then investigated their ability to activate cellular immune response. Indeed, these polymer-modified liposomes were shown to have capabilities of delivering antigenic OVA into cytosol of DCs and inducing antigen presentation through the MHC class I molecules on DCs. Nasal administration of these liposomes encapsulating OVA activated the antigen-specific cellular immunity in mice. Especially, highly fusogenic MGluPG liposomes exhibited high ability for CTL activation, which is comparable to the widely used adjuvant CFA. Despite its high ability to activate immune response, CFA is known to induce inflammatory reactions at the site of administration. Consequently, CFA is not applicable to humans. In contrast, MGluPG liposomes comprise phospholipid and biocompatible poly(glycidol) derivatives [27]. For that reason, MGluPG liposomes and their relevant liposomes might be promising antigen carriers for establishment of cancer immunotherapy and mucosal vaccination.

Acknowledgments

We are grateful to Dr. Clifford V. Harding (Department of Pathology, Case Western Reserve University, Cleveland, OH) for providing the CD8-OVA1.3 cells; to Dr. Judith A. Kapp (Department of Pathology, Emory University of School of Medicine, Atlanta, GA) for providing the OT4H.1D5 cells. This work was supported in part by a Grant-in-Aid for Research on Nano-technical Medicine from the Ministry of Health, Labor and Welfare of Japan and by a Grant-in-aid for Scientific Research from the Ministry of Education, Science, Sports, and Culture in Japan.

Appendix

Figures with essential colour discrimination. Certain figures in this article, in particular Figs. 1, 4 and 7, have parts that may be difficult to interpret in black and white. The full colour images can be found in the on-line version, at doi:10.1016/j.biomaterials.2009.10.006.

References

[1] Banchereau J, Steinman RM. Dendritic cells and the control of immunity. Nature 1998;392:245–52.
[2] Mellman I, Steinman RM. Dendritic cells: specialized and regulated antigen processing machines. Cell 2001;106:255–8.
[3] Fernadez NC, Lozier A, Flament C, Ricciardi-Castagnoli P, Bellet D, Suter M, et al. Dendritic cells directly trigger NK cell functions: cross-talk relevant in innate anti-tumor immune responses in vivo. Nat Med 1999;5:405–11.
[4] Akagi T, Wang X, Uto T, Baba M, Akashi M. Protein direct delivery to dendritic cells using nanoparticles based on amphiphilic poly(amino acid) derivatives. Biomaterials 2007;28:3427–36.
[5] Yoshikawa T, Okada N, Oda A, Matsuo K, Matsuo K, Mukai Y, et al. Development of amphiphilic γ-PGA-nanoparticulate cytosolic protein delivery carrier. Biochem Biophys Res Commun 2008;366:408–13.
[6] Kwon YJ, Standley SM, Goh SL, Fréchet JM. Enhanced antigen presentation and immunostimulation of dendritic cells using acid-degradable cationic nanoparticles. J Control Release 2005;105:199–212.
[7] Kunisawa J, Nakanishi T, Takahashi I, Okudaira A, Tsutsumi Y, Katayama K, et al. Sendai virus fusion protein mediates simultaneous induction of MHC class I/II-dependent mucosal and systemic immune responses via the nasopharyngeal-associated lymphoreticular tissue immune system. J Immunol 2001;167:1406–12.
[8] Bungener L, Serre K, Bijl L, Leserman L, Wilschut J, Daemen Y, et al. Virosome-mediated delivery of protein antigens to dendritic cells. Vaccine 2002;20:2287–95.
[9] Kono K, Igawa T, Takagishi T. Cytoplasmic delivery of calcein mediated by liposomes modified with a pH-sensitive poly(ethylene glycol) derivative. Biochim Biophys Acta 1997;1325:143–54.
[10] Sakaguchi N, Kojima C, Harada A, Kono K. Preparation of pH-sensitive poly(glycidol) derivatives with varying hydrophobicities: their ability to sensitize stable liposomes to pH. Bioconjugate Chemistry 2008;19:1040–8.
[11] Mestecky J, Michalek SM, Moldoveanu Z, Russell MW. Routes of immunization and antigen delivery systems for optimal mucosal immune responses in humans. Behring Inst Mitt 1997;98:33–43.
[12] Brennan FR, Bellaby T, Helliwell SM, Jones TD, Kamstrup S, Dalsgaard K, et al. Chimeric plant virus particles administered nasally or orally induce systemic and mucosal immune responses in mice. J Virol 1999;73:930–8.
[13] Sjolander S, Drane D, Davis R, Beezum L, Pearse M, Cox J. Intranasal immunisation with influenza-iscom induces strong mucosal as well as systemic antibody and cytotoxic T-lymphocyte responses. Vaccine 2001;19:4072–80.
[14] De Magistris MT. Mucosal delivery of vaccine antigens and its advantages in pediatrics. Adv Drug Del Rev 2006;58:52–67.
[15] Kono K, Zenitani K, Takagishi T. Novel pH-sensitive liposomes: liposomes bearing a poly(ethylene glycol) derivative with carboxyl groups. Biochim Biophys Acta 1994;1193:1–9.

[16] Shen Z, Reznikoff G, Dranoff G, Rock KL. Cloned dendritic cells can present exogenous antigens on both MHC class I and class II molecules. J Immunol 1997;158:2723–30.
[17] Moore MW, Carbone FR, Bevan MJ. Introduction of soluble protein into the class I pathway of antigen processing and presentation. Cell 1988;54:777.
[18] Harding CV, Song R. Phagocytic processing of exogenous particulate antigens by macrophages for presentation by class I MHC molecules. J Immunol 1994; 153:4925–33.
[19] Li Y, Ke Y, Gottlieb PD, Kapp JA. Delivery of exogenous antigen into the major histocompatibility complex class I and class II pathways by electroporation. J Leukoc Biol 1994;56:616–24.
[20] Lutz MB, Kukutsch N, Ogilvie AL, Rossner S, Koch F, Romani N, et al. An advanced culture method for generating large quantities of highly pure dendritic cells from mouse bone marrow. J Immunol Methods 1999;223:77–92.
[21] Kono K, Torikoshi Y, Mitsutomi M, Itoh T, Emi N, Yanagie H, et al. Novel gene delivery systems: complexes of fusogenic polymer-modified liposomes and lipoplexes. Gene Ther 2001;8:5–12.
[22] Struck DK, Hoekstra D, Pagano RE. Use of resonance energy transfer to monitor membrane fusion. Biochemistry 1981;20:4093–9.
[23] Yuba E, Kojima C, Sakaguchi N, Harada A, Koiwai K, Kono K. Gene delivery to dendritic cells mediated by complexes of lipoplexes and pH-sensitive fusogenic polymer-modified liposomes. J Controlled Release 2008;130: 77–83.
[24] Bergstrand N, Arfvidsson MC, Kim JM, Thompson DH, Edwards K. Interactions between pH-sensitive liposomes and model membranes. Biophys Chem 2003;104:361–79.
[25] Albert ML, Pearce SF, Francisco LM, Sauter B, Roy P, Silverstein RL, et al. Immature dendritic cells phagocytose apoptotic cells via alphavbeta5 and CD36, and cross-present antigens to cytotoxic T lymphocytes. J Exp Med 1998; 188:1359–68.
[26] Ke Y, Li Y, Kapp JA. Ovalbumin injected with complete Freund's adjuvant stimulates cytolytic responses. Eur J Immunol 1995;25:549–53.
[27] Kainthan RK, Janzen J, Levin E, Devine DV, Brooks DE. Biocompatibility testing of branched and linear polyglycidol. Biomacromolecules 2006;7:703–9.

ARTICLE IN PRESS
COREL-05399; No of Pages 9
Journal of Controlled Release xxx (2010) xxx–xxx
Contents lists available at ScienceDirect
Journal of Controlled Release
journal homepage: www.elsevier.com/locate/jconrel
NANOMEDICINE

Carboxylated hyperbranched poly(glycidol)s for preparation of pH-sensitive liposomes

Eiji Yuba [a], Atsushi Harada [a], Yuichi Sakanishi [b], Kenji Kono [a,*]

[a] Department of Applied Chemistry, Graduate School of Engineering, Osaka Prefecture University, 1-1 Gakuen-cho, Naka-ku, Sakai, Osaka 599-8531, Japan
[b] Daicel Chemical Industry, Ltd., 2-1-4, Higashisakae, Ohtake, Hiroshima 739-0695, Japan

ARTICLE INFO

Article history:
Received 19 November 2009
Accepted 1 March 2010
Available online xxxx

Keywords:
pH-sensitive liposome
Cytoplasmic delivery
Hyperbranched polymer
Membrane fusion
Dendritic cell

ABSTRACT

Previous reports by the authors described intracellular delivery using liposomes modified with various carboxylated poly(glycidol) derivatives. These linear polymer-modified liposomes exhibited a pH-dependent membrane fusion behavior in cellular acidic compartments. However, the effect of the backbone structure on membrane fusion activity remains unknown. Therefore, this study specifically investigated the backbone structure to obtain pH-sensitive polymers with much higher fusogenic activity and to reveal the effect of the polymer backbone structure on the interaction with the membrane. Hyperbranched poly(glycidol) (HPG) derivatives were prepared as a new type of pH-sensitive polymer and used for the modification of liposomes. The resultant HPG derivatives exhibited high hydrophobicity and intensive interaction with the membrane concomitantly with the increasing degree of polymerization (DP). Furthermore, HPG derivatives showed a stronger interaction with the membrane than the linear polymers show. Liposomes modified with HPG derivatives of high DP delivered contents into the cytosol of DC2.4 cells, a dendritic cell line, more effectively than the linear polymer-modified liposomes do. Results show that the backbone structure of pH-sensitive polymers affected their pH-sensitivity and interaction with liposomal and cellular membranes.

1. Introduction

Cytoplasmic delivery of bioactive molecules such as proteins and nucleic acids, which are unable to permeate a cellular membrane themselves, is important to establish therapies—such as immunotherapy and gene therapy—based on these molecules. Although various systems have been attempted for application to cytoplasmic delivery, one of the promising systems is pH-sensitive liposome, which induces destabilized and/or fusogenic activity under mildly acidic conditions. Various methods have been applied to produce pH-sensitive liposomes. For example, pH-sensitive amphiphiles, such as oleic acid and cholesteryl hemisuccinate, have been mixed with non-bilayer-forming phospholipid dioleoyl phosphatidylethanolamine (DOPE) to yield pH-sensitive liposomes [1,2]. Another efficient method for pH-sensitization of liposome is the modification of stable liposomes with pH-sensitive membrane active molecules such as fusion peptides derived from viral fusogenic proteins, or synthetic polymers with carboxyl groups such as poly(alkyl acrylic acid)s [3,4]. Earlier studies by the authors developed a series of carboxylated poly(glycidol) derivatives for pH-sensitization of liposomes [5–7]. These polymers have a linear backbone structure similar to that of poly(ethylene glycol) (PEG) and carboxyl groups on the side chains, which control the interaction of the polymer backbone with lipid membranes in a pH-dependent manner. Earlier studies showed that these polymer-modified liposomes are stable at neutral pH, but that they exhibit considerable destabilization under mildly acidic conditions and deliver contents into cytosol by membrane fusion with endosome/lysosome membranes [5–7].

Generally, membrane fusion as a biological function is mediated by fusogenic proteins. For example, enveloped viruses of various kinds have proteins that promote fusion of their envelope with cellular membranes to invade target cells. A very well studied viral fusion protein is influenza virus hemagglutinin (HA), which forms a fusion-active trimeric structure in the intracellular acidic compartment endosome and causes membrane fusion [8]. Considering these protein-mediated fusion processes, it might be important that fusogenic proteins having a bulky steric structure interact with a membrane for efficient membrane fusion because such interaction might generate a defective area and initiate membrane fusion.

Synthetic polymers of various kinds reportedly interact with membranes and induce membrane fusion [4,5,7,9,10]. Considering that these synthetic polymers generally have a linear structure, it is presumed that their interaction with membranes might not be so effective to generate defective regions for initiation of membrane fusion as sterically bulky proteins do. To date, the influence of the backbone structure of fusogenic polymers on their membrane fusion activity remains unknown. Hyperbranched polymers tend to take on a three-dimensional and spherical structure, which differs from those of

* Corresponding author. Tel./fax: +81 722 54 9330.
E-mail address: kono@chem.osakafu-u.ac.jp (K. Kono).

0168-3659/$ – see front matter © 2010 Elsevier B.V. All rights reserved.
doi:10.1016/j.jconrel.2010.03.001

linear polymers taking on a random coil structure [11–15]. Recently, 3-methyl-glutarylated poly(glycidol) was synthesized by the authors. It destabilizes phospholipid membranes under a weakly acidic environment and causes membrane fusion [7]. For the present study, its analogous polymers were prepared using hyperbranched poly(glycidol)s (HPGs) with different degrees of polymerization (DP), 3-methyl-glutarylated HPGs (MGlu-HPGs). Results described herein demonstrate that the DP and backbone structure of the pH-sensitive polymers affected their pH-sensitive fusion properties and their performance as intracellular delivery vehicles.

2. Materials and methods

2.1. Materials

HPGs with DPs of 10, 20, 40 and 60, which are respectively designated as HPG10, HPG20, HPG40 and HPG60, were provided by Daicel Chemical Industries, Ltd. (Osaka, Japan). Egg yolk phosphatidylcholine (EYPC) and L-dioleoyl phosphatidylethanolamine (DOPE) were kindly donated by NOF Co. (Tokyo, Japan). Pyrene, pyranine, 1-aminodecane and Triton X-100 were obtained from Tokyo Chemical Industries Ltd. (Tokyo, Japan). *p*-Xylene-bis-pyridinium bromide (DPX) was from Molecular Probes (Oregon, USA). *N*-(7-nitrobenz-2-oxa-1,3-diazol-4-yl)dioleoyl phosphatidylethanolamine (NBD-PE) and lissamine rhodamine B-sulfonyl phosphatidylethanolamine (Rh-PE) were purchased from Avanti Polar Lipids (Birmingham, AL, USA). 3-Methylglutaric anhydride was obtained from Aldrich (Milwaukee, WI). 4-(4,6-Dimethoxy-1,3,5-triazin-2-yl)-4-methyl morpholinium chloride (DMT-MM) was from Wako Pure Chemical Industries Ltd. (Osaka, Japan). Ovalbumin (OVA) and fluorescein isothiocyanate (FITC) were purchased from Sigma (St. Louis, MO.). 3-Methyl-glutarylated linear poly(glycidol) (MGluPG) (Fig. 1) was prepared as previously reported using two kinds of poly(glycidol)s with different molecular weights: PG76 with number average molecular weight (Mn) of 5.6×10^3 and weight average molecular weight (Mw) of 8.7×10^3, and PG222 with Mn of 1.6×10^4 and Mw of 2.5×10^4, which were evaluated using gel permeation chromatography with Shodex KD-803 and KF805L columns (Showa Denko) and poly (ethylene glycol)s as the standard. Obtained polymers were designated as MGluPG76 and MGluPG222, respectively [7]. FITC–OVA was prepared by reacting OVA (10 mg) with FITC (11.8 mg) in 0.5 M $NaHCO_3$ (4 mL, pH 9) at 4 °C for three days and subsequent dialysis.

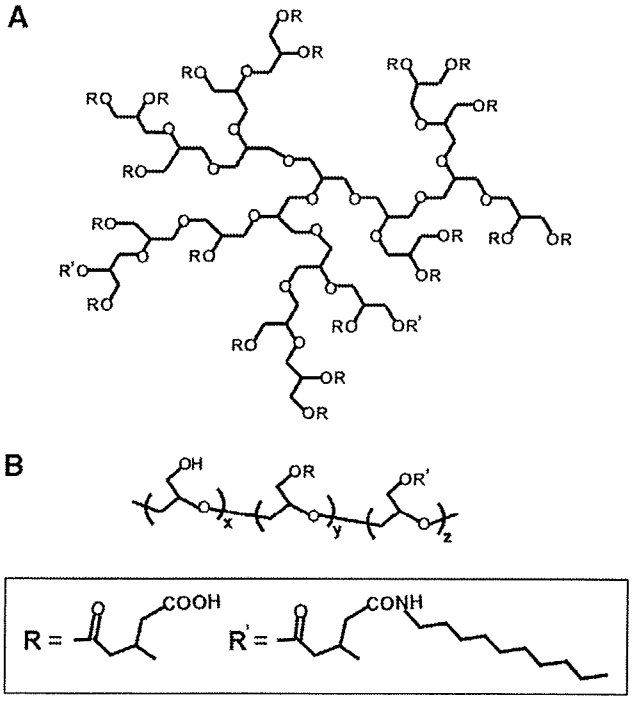

Fig. 1. Structures of MGlu-HPG20-C_{10} (A) and linear MGluPG-C_{10} (B).

2.2. Synthesis of hyperbranched poly(glycidol) derivatives

3-Methyl-glutarylated hyperbranched poly(glycidol) (MGlu-HPG) was prepared by reaction of HPG with varying DPs with 3-methylglutaric anhydride. HPG10 (0.765 g) and LiCl (0.765 g) were dissolved in pyridine (18 mL) and 3.0 equiv. of 3-methylglutaric anhydride (3.98 g) was added to the solution. The mixed solution was kept at 115 °C for 24 h with stirring. Then, the reaction mixture was evaporated and dialyzed against water for 3 days. The product was recovered by freeze-drying. HPG20, HPG40 and HPG60 were also reacted with 3-methylglutaric anhydride by the same procedure. As anchor moieties for fixation of MGlu-HPG onto liposome membranes, 1-aminodecane was combined with carboxyl groups of MGlu-HPG. Each polymer was dissolved in water around pH 7.4, and 1-aminodecane (0.18 equiv. to carboxyl group of polymer) was reacted to carboxyl groups of the polymer using DMT-MM (0.18 equiv. to carboxyl groups of polymers) at room temperature for three days with stirring. The obtained polymers were purified by dialysis in water.

2.3. Cell culture

DC2.4 cells, which were an immature murine dendritic cell (DC) line, were provided from Dr. K. L. Rock (Harvard Medical School, USA) and were grown in RPMI 1640 supplemented with 10% FBS (MP Biomedical, Inc.), 2 mM L-glutamine, 100 μM non-essential amino acids (Gibco, Inc.), 50 μM 2-mercaptoethanol (2-ME) and antibiotics at 37 °C [16].

2.4. Precipitation pH

Precipitation pH of polymers was determined by measuring the optical density of aqueous polymer solutions (0.25 mg/mL) at various pHs. Polymers were dissolved in 30 mM sodium acetate and 120 mM NaCl aqueous solution of various pHs. After 5 min-incubation at 25 °C, optical densities of the polymer solutions at 500 nm were measured by using a spectrophotometer (Jasco V-520). Precipitation pH was determined using optical density–pH profiles as the pH at which OD drastically rose.

2.5. Pyrene fluorescence

A given amount of pyrene in acetone solution was added to an empty flask, and acetone was removed under vacuum. Polymer (0.2 mg/mL) dissolving in 25 mM MES and 125 mM NaCl solution of a given pH was added to the flask, yielding 1 μM concentration of pyrene. The sample solution was stirred overnight at room temperature, and emission spectra with excitation at 337 nm were recorded. The fluorescence intensity ratio of the first band at 373 nm to the third band at 384 nm (I_1/I_3) was analyzed as a function of pH of the solution.

2.6. Preparation of pyranine-loaded liposomes

500 μL of aqueous 35 mM pyranine, 50 mM DPX, and 25 mM MES solution (pH 7.4) were added to a dry, thin membrane of EYPC (7 mg), and the mixture was sonicated for 2 min using a bath-type sonicator. The liposome suspension was further hydrated by freezing and thawing, and was extruded through a polycarbonate membrane with a pore size of 100 nm. The liposome suspension was applied to a

Please cite this article as: E. Yuba, et al., Carboxylated hyperbranched poly(glycidol)s for preparation of pH-sensitive liposomes, J. Control. Release (2010), doi:10.1016/j.jconrel.2010.03.001

sepharose4B column to remove free pyranine from the pyranine-loaded liposomes. Polymer-modified liposomes were also prepared according to the above procedure using dry membranes of mixtures of EYPC and various polymers (EYPC/polymer = 7/3, w/w).

2.7. Release of pyranine from liposome

Release of pyranine from liposome was measured as previously reported [7,17]. Pyranine fluorescence was quenched by DPX inside of the liposomes, but this molecule exhibits intense fluorescence when released from the liposome [17]. For the study of the interaction of polymers with lipid membranes, a given amount of the polymer dissolved in the same buffer (final concentration: 0.013 mg/mL) at 25 °C was added to a suspension of pyranine-loaded liposomes (lipid concentration: 2.0×10^{-5} M) in 25 mM MES and 125 mM NaCl buffer of varying pHs,, and fluorescence intensity (512 nm) of the mixed suspension was followed with excitation at 416 nm using a spectrofluorometer (Jasco FP-6500). For the study of the release behavior of polymer-modified liposomes, polymer-modified liposomes encapsulating pyranine were added to 25 mM MES and 125 mM NaCl buffer of varying pHs at 37 °C and fluorescence intensity of the suspension was monitored (lipid concentration: 2.0×10^{-5} M). The percent release of pyranine from liposomes was defined as

$$\text{Release}(\%) = (F_t - F_i) / (F_f - F_i) \times 100$$

where F_i and F_t mean the initial and intermediary fluorescence intensities of the liposome suspension, respectively. F_f is the fluorescent intensity of the liposome suspension after the addition of TritonX-100 (final concentration: 0.1%).

2.8. Liposome size change

EYPC liposomes were prepared as described above without pyranine and DPX. EYPC liposomes (4.1 mM, 103.4 μL, pH 7.4) were added to 25 mM MES and 125 mM NaCl buffer of various pHs (2370 μL). And then, 26.6 μL of polymer solution of the same buffer (10 mg/mL, pH 7.4) was added. The mixed solutions were incubated overnight. pH of the mixed solution was measured and liposome diameters were evaluated using a Nicomp 380 ZLS dynamic light scattering instrument (Particle Sizing Systems, Santa Barbara, CA) equipped with a 35 mW laser (λ = 632.8 nm). Data were obtained as an average of more than three measurements on different samples.

2.9. Intracellular behavior of liposomes

The FITC–OVA-loaded liposomes containing Rh-PE were prepared as described above except that mixtures of polymers and EYPC containing Rh-PE (0.1 mol%) were dispersed in phosphate-buffered saline containing FITC–OVA (4 mg/mL). The DC2.4 cells (2×10^5 cells) cultured for 2 days in 35-mm glass-bottom dishes were washed with Hank's balanced salt solution (HBSS, Sigma), and then incubated in serum-free RPMI medium (500 μL). The FITC–OVA-loaded liposomes (100 μg/mL of FITC–OVA, 500 μL) were added gently to the cells and incubated for 4 h at 37 °C. After the incubation, the cells were washed with HBSS three times. Confocal laser scanning microscopic (CLSM) analysis of these cells was performed using LSM 5 EXCITER (Carl Zeiss Co. Ltd.). Fluorescence intensity of these cells was also determined using a Coulter Epics XL Flow Cytometer (Coulter Corporation, Florida, USA) [18].

2.10. Fusion of liposomes in cell

Liposomes containing NBD-PE and Rh-PE (each 0.6 mol%) were prepared as described above using DOPE as an additional lipid component and suspended in PBS. The DC2.4 cells (2×10^5 cells) cultured for 2 days in 35-mm glass-bottom dishes were washed with HBSS, and then incubated in serum-free RPMI medium (500 μL). Then, the liposome suspensions (1.0 mM of liposomal lipid, 500 μL) were added gently to the medium of the cells and incubated for 4 h at 37 °C. After the incubation, the cells were washed with HBSS three times and analyzed by CLSM. Fluorescence of NBD-PE and Rh-PE was observed through specific path filters (λ_{em} = 500–530 nm for NBD-PE and λ_{em} > 560 nm for Rh-PE) with excitation at 488 nm. Fluorescence intensities of these cells were also determined by flow cytometry with excitation at 488 nm. The fluorescence intensity ratio of NBD-PE to Rh-PE was defined as

$$\text{NBD / Rh} = (I_{NBD} - I_{NBD,0}) / (I_{Rh} - I_{Rh,0})$$

where I_{NBD} and I_{Rh} are the fluorescence intensities of the liposome-treated cells detected by FL1 (λ_{em} = 505–545 nm) and FL2 channel (λ_{em} = 560–590 nm), respectively. $I_{NBD,0}$ and $I_{Rh,0}$ are the fluorescence intensities of untreated cells detected by FL1 and FL2 channel, respectively.

3. Results and discussion

3.1. Characterization of HPG derivatives

Previous studies developed and assessed a series of carboxylated linear poly(glycidol) derivatives for pH-sensitization of liposome [5–7]. Especially, MGluPG-modified liposomes were stable at neutral pH and showed strong fusogenic activity under weakly acidic conditions [7]. Considering the function of viral fusogenic proteins for viral membrane fusion, it was assumed that a polymer with a three-dimensional backbone structure can interact with membranes more effectively and intensively than a linear polymer. Therefore, a hyperbranched polymer was selected as a backbone structure. We prepared four kinds of MGlu-HPGs with different molecular sizes, namely MGlu-HPG10, MGlu-HPG20, MGlu-HPG40, and MGlu-HPG60, using HPGs with DPs of 10, 20, 40, and 60, as pH-sensitive polymers with a hyperbranched structure. Also, two kinds of MGluPGs with different chain lengths, namely MGluPG76 and MGluPG222, were prepared as pH-sensitive polymers with a linear structure, using PG76 and PG222. Hydrodynamic diameters of HPG10, HPG20, HPG40, HPG60, PG76, and PG222 were estimated to be 2.0, 2.6, 3.2, 3.6, 4.8, and 8.6 nm, respectively, according to the method of Hester and Mitchell using GPC with PEG standards [19].

Compositions of these polymers, which were estimated using ^{1}H NMR, are presented in Table 1. For all polymers, only low percentages of unreacted glycidol units remained on the polymer backbone after the reaction of HPG with 3-methylglutaric anhydride, demonstrating the high efficiency of these reactions, which is consistent with a previous report [7]. Fundamentally, every repeating unit possesses a carboxyl group in the resultant polymers. Results of an earlier study showed that attachment of 1-aminodecane to about 8 unit% of a

Table 1
Compositions of various hyperbranched and linear poly(glycidol) derivatives.

Polymer	Hydroxyl unit/%	Carboxylated unit/%	Anchor unit/%
MGlu-HPG10	0	100	–
MGlu-HPG20	0	100	–
MGlu-HPG40	0	100	–
MGlu-HPG60	5	95	–
Linear MGluPG76	10	90	–
Linear MGluPG222	6	94	–
MGlu-HPG10-C_{10}	0	88	12
MGlu-HPG20-C_{10}	0	90	10
MGlu-HPG40-C_{10}	0	90	10
MGlu-HPG60-C_{10}	5	85	10
Linear MGluPG76-C_{10}	10	75	15
Linear MGluPG222-C_{10}	9	81	10

Please cite this article as: E. Yuba, et al., Carboxylated hyperbranched poly(glycidol)s for preparation of pH-sensitive liposomes, J. Control. Release (2010), doi:10.1016/j.jconrel.2010.03.001

carboxylated poly(glycidol) chain is sufficient to fix the polymer chain onto an EYPC liposome membrane [5,7]. Based on previous studies, 1-aminodecane was combined to about 10 unit% of the polymer chains in this study (Table 1).

Acid–base titration of these polymers was performed to estimate the p*K*a values. As presented in Table 2, MGlu-HPGs had p*K*a values around 5.9–6.5 and p*K*a slightly increased concomitantly with increasing DP. For polymers with a hyperbranched structure, their chain density increases concomitantly with increasing DP. Therefore, hydrophobic interactions among these crowded polymer chains of HPG with higher DP might engender a more compact conformation. Such a compact conformation of HPGs increases spatial density of carboxyl groups in the polymer chains, which might suppress dissociation of carboxyl groups to avoid repulsive electrostatic forces among carboxylate anions. In addition, hydrophobic environment of the crowded polymer chains may induce suppression of dissociation of carboxyl groups. As a result, p*K*a of the MGlu-HPGs might increase with increasing DP.

Hydrophobicity of carboxylated polymers affects their precipitation behaviors [20]. For that reason, we estimated the pH at which the polymers precipitate by measuring optical densities of these polymer solutions at varying pHs (Fig. 2). These polymers were soluble in water at neutral pH; their solutions were transparent. However, the polymer solutions suddenly became turbid at a specific pH, which was defined as the precipitation pH. The precipitation pH thresholds for MGlu-HPGs were estimated as presented in Table 2. The precipitation pH shifted to slightly higher pH values with increasing DP of MGlu-HPGs, indicating that hydrophobicity of MGlu-HPG increases concomitantly with increasing DP, consistent with previous observations for methacrylic acid copolymers with varying hydrophobicities and a previous report by the authors [7,20]. Acid–base titration for these polymers revealed that the degree of protonation for their carboxyl groups was around 0.94–0.99 at the precipitation pH: most carboxyl groups must be protonated to elicit precipitation of these polymers.

Hydrophobicity of the polymers was further investigated using a fluorescence probe pyrene. An emission intensity ratio of the first (373 nm) to the third (384 nm) peaks of pyrene, I_1/I_3, is known to be sensitive to the micro-environmental polarity surrounding the pyrene molecule [21]. Consequently, this ratio has been widely used to estimate the hydrophobic nature of polymers [22,23]. Fig. 3 depicts the I_1/I_3 ratio of pyrene fluorescence in the buffer dissolving various polymers as a function of pH. In buffers dissolving MGlu-HPG10 or MGlu-HPG20, the I_1/I_3 ratios of pyrene were around 1.75 at pH 5, suggesting that these polymers formed few domains with a hydrophobic nature, even after protonation of carboxyl groups of the polymer chain. On the other hand, a significant decrease in the I_1/I_3 ratio is seen in the presence of MGlu-HPG40 or MGlu-HPG60 under weakly acidic conditions. These results suggest that MGlu-HPGs with higher DP formed more hydrophobic domains probably because of their globular structure. The presence of linear MGluPGs also affected the I_1/I_3 ratio, which tends to decrease below pH 6.0. However, their I_1/I_3 values were generally higher than those of MGlu-HPGs with similar DP. Linear MGluPGs might be unable to form hydrophobic domains as much as MGlu-HPGs because of their linear backbone structure.

Table 2
p*K*a and precipitation pH of various hyperbranched and linear poly(glycidol) derivatives.

Polymer	p*K*a	Precipitation pH	Degree of protonation at precipitation pH
MGlu-HPG10	5.9	4.4	0.98
MGlu-HPG20	6.2	4.6	0.98
MGlu-HPG40	6.5	4.7	0.99
MGlu-HPG60	6.5	4.9	0.94
Linear MGluPG76	6.2	4.9	0.99

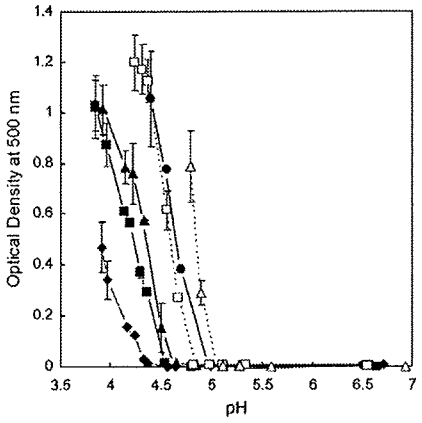

Fig. 2. Optical densities at 500 nm for solutions of MGlu-HPG10 (closed diamonds), MGlu-HPG20 (closed squares), MGlu-HPG40 (closed triangles), MGlu-HPG60 (closed circles), linear MGluPG76 (open triangles), and linear MGluPG222 (open squares) dissolved in 30 mM sodium acetate and 120 mM NaCl of various pHs (0.25 mg/mL) at 25 °C. Each point is the mean ± SD ($n = 3$).

3.2. Interaction of HPG derivatives with lipid membrane

We have shown that anchoring moiety into liposomes was necessary for poly(glycidol) derivatives to interact with liposomal membrane [7]. MGlu-HPG with anchor moieties (MGlu-HPG-C_{10}) were added to liposomes encapsulating both pyranine and its quencher DPX, and fluorescence of the released pyranine was monitored (Fig. 4). At neutral pH, no polymer showed a content release (Fig. 4A), indicating that these polymers did not disrupt liposome membrane under this condition. On the other hand, release of the contents was observed for all MGlu-HPG-C_{10} at pH 6.5 (Fig. 4B). Complete release was achieved below pH 6.0 (Fig. 4C), indicating that protonated polymers disrupt the liposome membrane. As portrayed in Fig. 4D, the content release in the weakly acidic region increased in the order of DP of MGlu-HPGs-C_{10}, indicating that the polymer with higher hydrophobicity triggers release more strongly. In addition, MGlu-HPGs-C_{10} triggered the content release more strongly

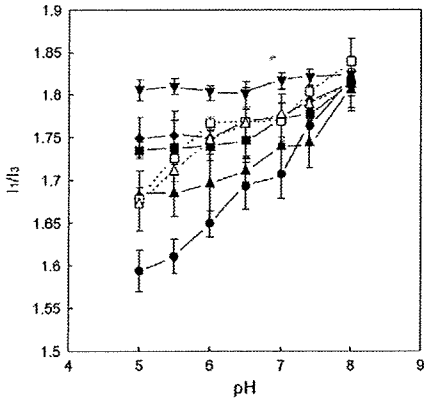

Fig. 3. pH-Dependence of I_1/I_3 of pyrene fluorescence in the absence (closed inverted triangles) or presence of MGlu-HPG10 (closed diamonds), MGlu-HPG20 (closed squares), MGlu-HPG40 (closed triangles), MGlu-HPG60 (closed circles), linear MGluPG76 (open triangles), and linear MGluPG222 (open squares) dissolving in 25 mM MES and 125 mM NaCl solution. Concentration of polymers and pyrene were 0.2 mg/mL and 1 μM, respectively. I_1/I_3 was defined as the fluorescence intensity ratio of the first band at 373 nm to the third band at 384 nm.

Please cite this article as: E. Yuba, et al., Carboxylated hyperbranched poly(glycidol)s for preparation of pH-sensitive liposomes, J. Control. Release (2010), doi:10.1016/j.jconrel.2010.03.001

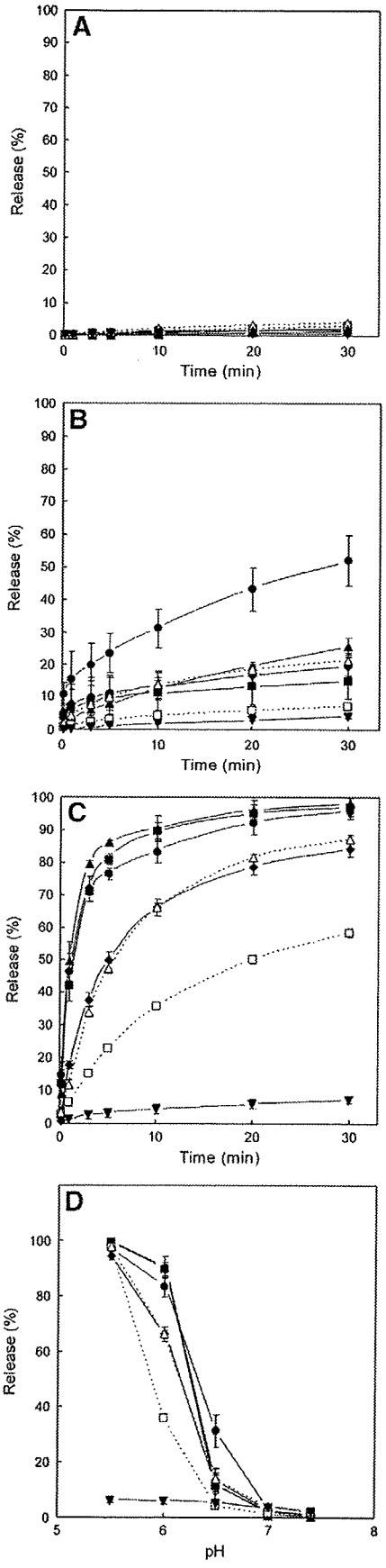

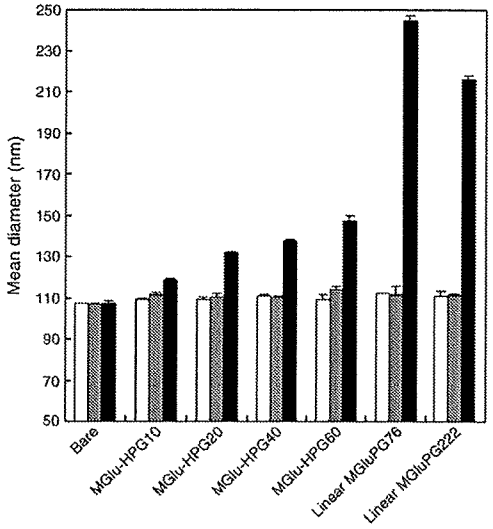

Fig. 5. Mean diameters of EYPC liposomes after overnight incubation with various polymers or without polymer at pH 7.4 (open bars), pH 6.5 (gray bars) and pH 5.5 (closed bars). Polymer and lipid concentrations were 0.11 mg/mL and 1.7×10^{-4} M, respectively. Each point is the mean ± SD ($n=3$).

than linear MGluPG-C_{10} under the weakly acidic condition, demonstrating that the hyperbranched polymers can destabilize the liposome membrane more strongly than linear polymers.

Interaction of the polymers with the liposomes was also investigated through inspection of the liposome size change. EYPC liposomes were incubated with MGlu-HPGs-C_{10} or linear MGluPGs-C_{10} at various pHs overnight; their diameters were evaluated by DLS (Fig. 5). The liposome size changed only slightly after incubation with MGlu-HPGs-C_{10} at pHs 7.4 and 6.5, but incubation at pH 5.5 increased their diameter to some extent. This range of increase rose with increasing DP. On the other hand, incubation with linear MGluPGs-C_{10} induced remarkable liposome size change at pH 5.5. Because linear MGluPG-C_{10} has a high degree of freedom on their conformation, they might promote intervesicular interaction, engendering aggregation of liposomes. In contrast, MGlu-HPGs-C_{10} might interact with the membrane in a single liposome because of their compact conformation.

3.3. Preparation of pH-sensitive liposomes using HPG derivatives

Fig. 6 depicts pH-sensitive content release behaviors of liposomes modified with MGlu-HPGs-C_{10} or linear MGluPGs-C_{10}. All liposomes retained pyranine at pH 7.4 (Fig. 6A). However, MGlu-HPGs-C_{10}-modified liposomes enhanced their content release below pH 6.0; an almost complete release was achieved at pH 5.5 (Fig. 6B and C). As portrayed in Fig. 6D, liposomes modified with MGlu-HPGs-C_{10} of low DP exhibited higher content release in acidic pH than MGlu-HPGs-C_{10} of high DP. These observations differ from the case of content release induced by the addition of these polymers into the liposome suspensions (Fig. 4). These might be resulted from the difference of protonation behavior of polymers between the liposome surface and in an aqueous medium. It is possible that the protonation of MGlu-HPG-C_{10} with low DP is enhanced on the

Fig. 4. Pyranine release from EYPC liposomes induced by various hyperbranched poly (glycidol) derivatives. Time courses at pH 7.4 (A), pH 6.5 (B), and pH 6.0 (C), and pH-dependence (D) of pyranine release induced by MGlu-HPG10 (closed diamonds), MGlu-HPG20 (closed squares), MGlu-HPG40 (closed triangles), MGlu-HPG60 (closed circles), linear MGluPG76 (open triangles), and linear MGluPG222 (open squares) or without polymer (closed and inverted triangles). Percent release of pyranine after 10 min-incubation was shown (D). Polymer and lipid concentrations were 0.013 mg/mL and 2.0×10^{-5} M, respectively. Each point is the mean ± SD ($n=3$).

Please cite this article as: E. Yuba, et al., Carboxylated hyperbranched poly(glycidol)s for preparation of pH-sensitive liposomes, J. Control. Release (2010), doi:10.1016/j.jconrel.2010.03.001

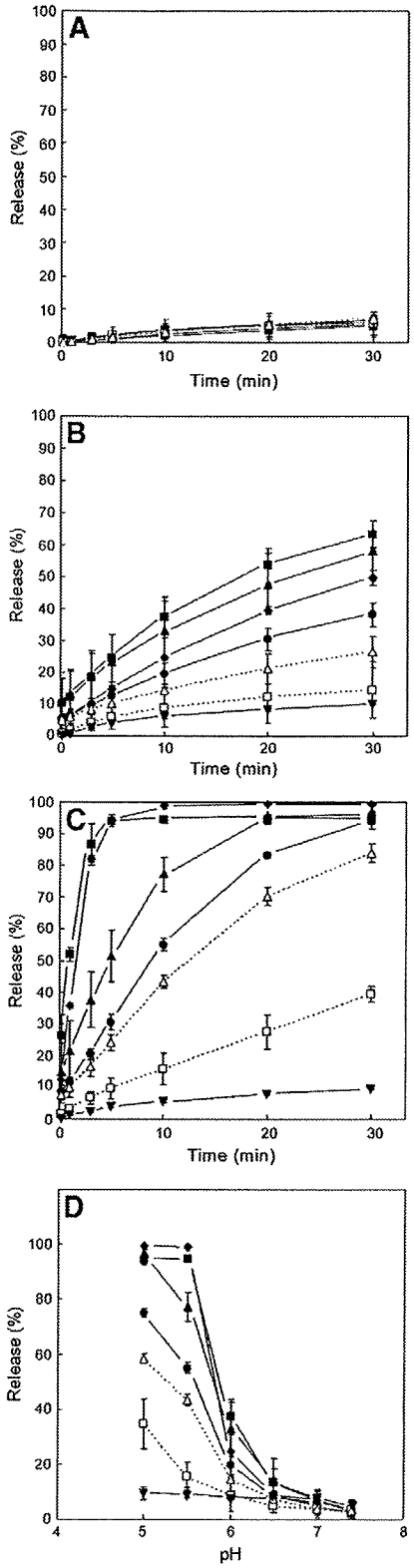

Fig. 6. Pyranine release from EYPC liposomes modified with various hyperbranched and linear poly(glycidol) derivatives. Time courses at pH 7.4 (A), pH 6.0 (B), and pH 5.5 (C), and pH-dependence (D) of pyranine release from EYPC liposomes modified with MGlu-HPG10 (closed diamonds), MGlu-HPG20 (closed squares), MGlu-HPG40 (closed triangles), MGlu-HPG60 (closed circles), linear MGluPG76 (open triangles), linear MGluPG222 (open squares), and unmodified EYPC liposomes (closed and inverted triangles). Percent release of pyranine after 10 min-incubation was shown (D). Lipid concentrations were 2.0×10^{-5} M. Each point is the mean ± SD ($n=3$).

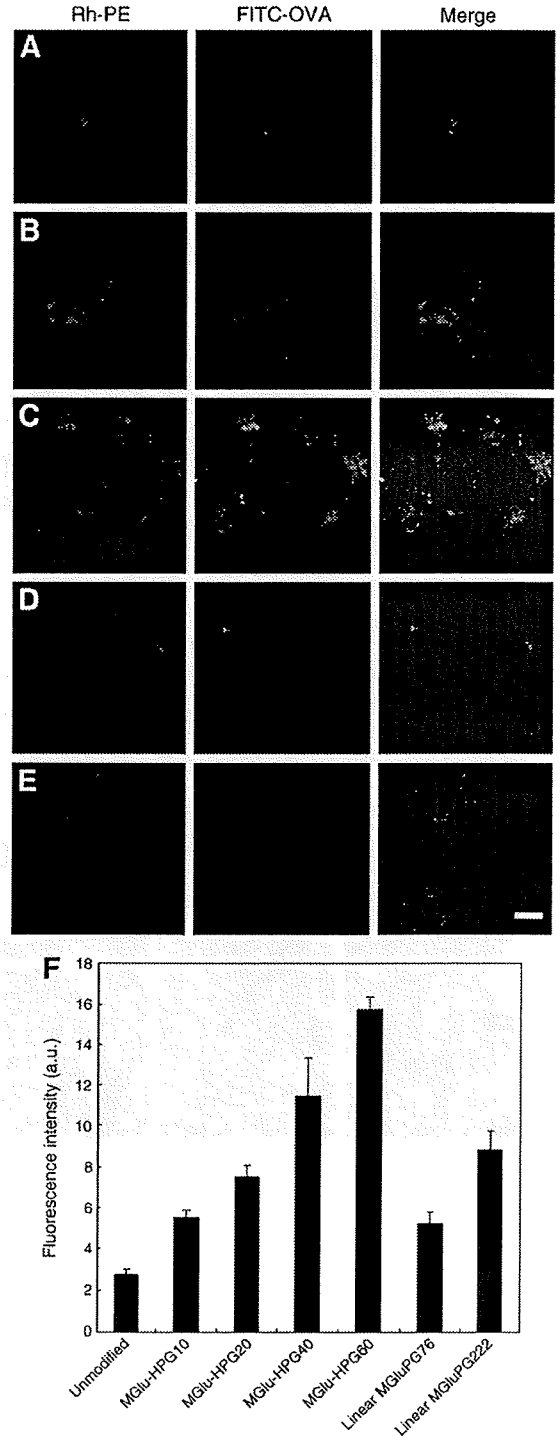

Fig. 7. Confocal laser scanning microscopic (CLSM) images of DC2.4 cells treated with Rh-PE-labeled and FITC-OVA-loaded EYPC liposomes of various types: plain liposomes (A); liposomes modified with MGlu-HPG20-C_{10} (B), MGlu-HPG60-C_{10} (C), linear MGluPG76-C_{10} (D), or linear MGluPG222-C_{10} (E). FITC-OVA concentration was 50 μg/mL. Intracellular localization of Rh-PE (red) and FITC-OVA (green) was observed using a CLSM. Scale bar represents 10 μm. (F) Fluorescence intensities of DC2.4 cells treated with Rh-PE-labeled EYPC liposomes modified with or without polymers of various types. The fluorescence intensities of Rh-PE were determined by flow cytometry. (For interpretation of the references to color in this figure legend, the reader is referred to the web version of this article.)

Please cite this article as: E. Yuba, et al., Carboxylated hyperbranched poly(glycidol)s for preparation of pH-sensitive liposomes, J. Control. Release (2010), doi:10.1016/j.jconrel.2010.03.001

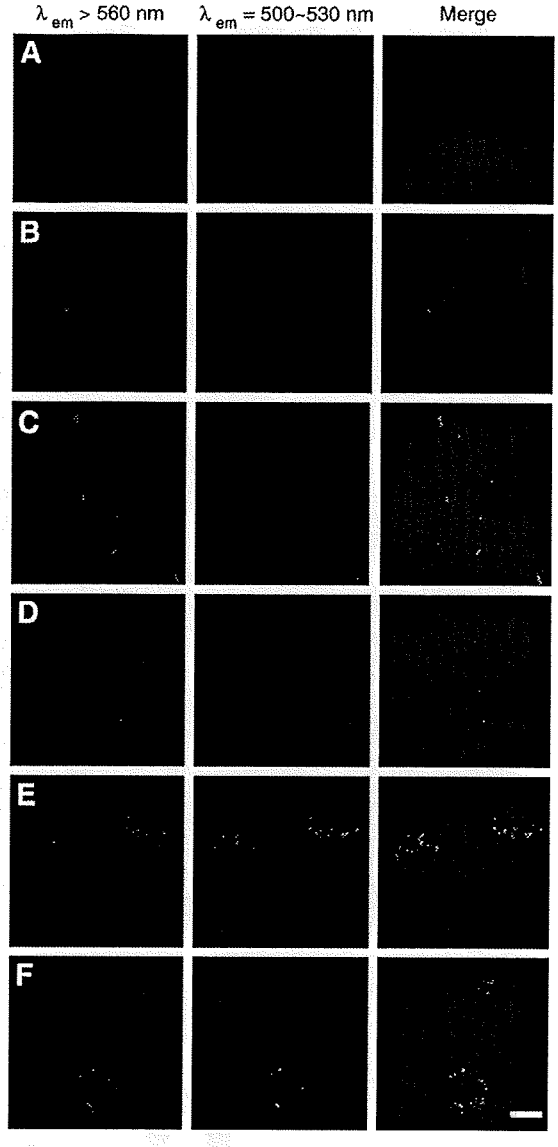

liposome membrane because carboxylate anions of the small-size polymer might exist in close vicinity of the membrane. Comparison of liposomes modified with linear and hyperbranched polymers shows that MGlu-HPG-C_{10}-modified liposomes induced the content release in a higher pH region than linear MGluPG-C_{10}-modified liposomes. Therefore, the liposomes having the hyperbranched polymers might destabilize the endosome in the early stage of endocytic pathway after their uptake by a cell.

3.4. Cytoplasmic delivery by polymer-modified liposomes

Previously, we have shown that liposomes modified with linear MGluPG can be used for cytoplasmic delivery of antigenic proteins, such as OVA, into dendritic cells for the induction of antigen-specific immune responses [24]. Therefore, we compared the performance of the MGlu-HPG-modified liposomes as antigenic protein delivery vehicles with that of the linear MGluPG-modified liposomes.

We prepared the MGlu-HPGs-C_{10}-modified liposomes labeled with Rh-PE and loaded with FITC–OVA, and their interaction with DC2.4 cells was compared with that for the linear MGluPG-C_{10}-modified EYPC liposomes or bare EYPC liposomes labeled with Rh-PE and loaded with FITC–OVA. As presented in Fig. 7A, cells treated with the bare liposome displayed weak and punctate fluorescence of Rh-PE and FITC–OVA. Considering that the liposomes were generally taken up by a cell *via* endocytosis, it is highly likely that FITC–OVA molecules were still trapped in the endosome and/or lysosome. In contrast, cells treated with MGlu-HPG-C_{10}-modified liposomes showed punctate fluorescence of Rh-PE but diffuse fluorescence of FITC–OVA (Fig. 7B and C), indicating that lipid molecules existed in the endosome and lysosome but that FITC–OVA molecules existed in the cytoplasm. These liposomes have the capability of destabilizing lipid membranes under a weakly acidic environment. Therefore, it is likely that FITC–OVA molecules were transferred from the endosome into the cytoplasm. Furthermore, the fluorescence from cells treated with MGlu-HPG60-C_{10}-modified liposomes was much brighter than that from cells treated with MGlu-HPG20-C_{10}. Although diffuse fluorescence of FITC–OVA was also observed for cells treated with the linear MGluPG-C_{10}-modified liposomes (Fig. 7D and E), their fluorescence was weaker than the case of MGlu-HPG60-C_{10}-modified liposomes.

The Rh-fluorescence intensity of the liposome-treated cells was evaluated by flow cytometry (Fig. 7F). The Rh-fluorescence intensity increased concomitantly with increasing DP of MGlu-HPGs-C_{10}, indicating that liposomes modified with MGlu-HPG-C_{10} of higher DP were taken up more efficiently. In addition, cells treated with the MGlu-HPG60-C_{10}-modified liposomes showed higher intensity than those treated with the linear MGluPGs-C_{10}-modified liposomes. This result suggests that liposomes having polymers of a hyperbranched structure were taken up by cells more efficiently than those with the polymers of a linear structure. We have shown that linear MGluPG-modified liposomes are taken up by DC2.4 cells through their interaction with the cellular scavenger receptors, which recognize carboxylate anions of polymers [18,24]. Negatively charged carboxylate groups of the hyperbranched polymer tend to locate in the peripheral region of the polymer. Therefore, these groups might be recognized by scavenger receptors efficiently, thereby promoting their uptake by the cells. These results demonstrate that modification

Fig. 8. CLSM images of DC2.4 cells treated with EYPC (A–C) or EYPC/DOPE (1/1, mol/mol) (D–F) plain liposomes (A, D) or liposomes modified with MGlu-HPG60-C_{10} (B, E), and linear MGluPG76-C_{10} (C, F). Liposomal lipid concentration was 0.5 mM. Fluorescence of NBD-PE and Rh-PE upon excitation at 488 nm was observed using a CLSM. Scale bar represents 10 μm. (G) Fluorescence intensity ratios of NBD-PE to Rh-PE for DC2.4 cells treated with EYPC (closed symbols) or EYPC/DOPE (open symbols) liposomes modified with or without polymers. Fluorescence intensity ratios were evaluated by flow cytometry and were expressed as relative values using the ratio of the plain EYPC liposome-treated cells as the standard.

Please cite this article as: E. Yuba, et al., Carboxylated hyperbranched poly(glycidol)s for preparation of pH-sensitive liposomes, J. Control. Release (2010), doi:10.1016/j.jconrel.2010.03.001

of liposomes with MGlu-HPG-C_{10} can produce pH-sensitive liposomes that achieve efficient cytoplasmic delivery of proteins.

3.5. Fusion of polymer-modified liposomes within cell

Finally, we attempted to verify the fusion of MGlu-HPG-C_{10}-modified liposomes in the cells. The polymer-modified liposomes containing NBD-PE and Rh-PE were prepared to detect the fusion of the liposomes with intracellular membranes [6,25]. Fusion of the labeled liposomes with endosomal membranes causes dilution of these fluorescent lipids in the membrane, resulting in a decrease of energy transfer efficiency between these fluorescent lipids.

The fluorescent lipid-labeled liposomes with or without polymers were applied to DC2.4 cells and incubated for 4 h. Then cellular fluorescence was observed using a CLSM under irradiation of light with a wavelength of 488 nm, which is for excitation of NBD-PE (Fig. 8). As Fig. 8A shows, cells treated with the bare liposomes displayed only the fluorescence of Rh-PE, suggesting that the fluorescence of NBD-PE was quenched by energy transfer to Rh-PE and hence the bare liposomes did not fuse with the endosomal membrane. In contrast, the cells treated with MGlu-HPG60-C_{10}-modified or linear MGluPG76-C_{10}-modified liposomes exhibited not only Rh-PE-fluorescence but also NBD-PE-fluorescence, indicating that the fusion between these liposomes and the endosomal membranes occurred (Fig. 8B and C). However, the fluorescence of NBD-PE was very weak, suggesting that their fusion was not efficient.

The intracellular fusion behavior of the liposomes containing a non-bilayer-forming lipid DOPE, which is known to enhance membrane fusion, was also examined (Figs. 8D–F). For cells treated with the bare EYPC/DOPE liposomes, fluorescence of NBD-PE remained very weak (Fig. 8D). However, intensive fluorescence of NBD-PE was detected from cells treated with the DOPE-containing liposomes having either MGlu-HPG60-C_{10} or linear MGluPG76-C_{10}, indicating that these polymer-modified liposomes fused efficiently with endosomal membranes (Figs. 8E and F).

The fluorescence intensity ratios of NBD-PE to Rh-PE for the liposome-treated cells were evaluated by flow cytometry and were expressed as relative values using the ratio of the bare EYPC liposome-treated cells as the standard (Fig. 8G). The cells treated with either polymer-modified EYPC liposomes showed a 2–3 times increase in the NBD/Rh ratio compared with those treated with the base EYPC liposomes. Furthermore, no significant difference was found between the cells treated with any MGlu-HPG-C_{10}-modified and linear MGluPG-C_{10}-modified EYPC liposomes. These results indicate that these polymer-modified EYPC liposomes possess similar abilities to fuse with the endosomal membrane. Indeed, the EYPC/DOPE liposomes modified with these polymers caused a more significant increase in the NBD/Rh ratio than EYPC liposomes having the same polymers (Fig. 8G). In particular, the EYPC/DOPE liposomes modified with the hyperbranched polymers showed a higher NBD/Rh ratio than linear polymers, indicating that the backbone structure of the polymer affects their ability to generate the fusion ability of EYPC/DOPE liposomes.

The performance of MGlu-HPG-modified liposomes as a cytoplasmic delivery system was shown to increase as MGlu-HPG with higher DP was used for liposome modification. There might be various modes of interaction between MGlu-HPG with lipid membranes, such as absorption onto the membrane, penetration into the membrane, and solubilization lipid molecules. Therefore, their ability to destabilize lipid membranes might be influenced by their size. Optimization of molecular size may generate MGlu-HPG-modified liposomes with even higher performance.

4. Conclusion

A new type of pH-sensitive polymer with a hyperbranched backbone—MGlu-HPG-C_{10}—was synthesized. Its feasibility for the production of pH-sensitive liposomes was then investigated. Their ability for pH-sensitization of liposomes was enhanced with increasing DP. Modification of liposomes with MGlu-HPG-C_{10} produced highly pH-sensitive liposomes that undergo content release at mildly acidic pH. The MGlu-HPG-C_{10}-modified liposomes encapsulating OVA delivered their contents efficiently into the cytosol of DC2.4 cells. Especially, liposomes having MGlu-HPG-C_{10} with high DP exhibited higher fusion ability and more efficient cellular internalization property than the liposomes modified with the counterpart polymers with a linear backbone structure. This is the first report describing the importance of the polymer backbone structure for polymer-based functionalization of liposomes. The MGlu-HPG-C_{10}-modified liposomes showed an excellent ability to deliver the loaded proteins into the cytosol of dendritic cell-derived cells. Therefore, they might have potential usefulness for the delivery of antigenic proteins.

Acknowledgments

This work was supported in part by a Grant-in-Aid for Research on Nanotechnical Medicine from the Ministry of Health, Labor and Welfare of Japan and by a Grant-in-aid for Scientific Research from the Ministry of Education, Science, Sports, and Culture in Japan. E. Yuba thanks the Research Fellowships of the Japan Society for the Promotion of Science for Young Scientists.

References

[1] D. Liu, L. Huang, pH-Sensitive, plasma-stable liposomes with relatively prolonged residence in circulation, Biochim. Biophys. Acta 1022 (1990) 348–354.
[2] H. Ellens, J. Bentz, F.C. Szoka, pH-Induced destabilization of phosphatidylethanolamine-containing liposomes: role of bilayer contact, Biochemistry 23 (1984) 1532–1538.
[3] J. Kunisawa, T. Nakanishi, I. Takahashi, A. Okudaira, Y. Tsutsumi, K. Katayama, S. Nakagawa, H. Kiyono, T. Mayumi, Sendai virus fusion protein mediates simultaneous induction of MHC class I/II-dependent mucosal and systemic immune responses via the nasopharyngeal-associated lymphoreticular tissue immune system, J. Immunol. 167 (2001) 1406–1412.
[4] K. Seki, D.A. Tirrell, pH-Dependent complexation of poly(acrylic acid) derivatives with phospholipid vesicle membrane, Macromolecules 17 (1984) 1692–1698.
[5] K. Kono, K. Zenitani, T. Takagishi, Novel pH-sensitive liposomes: liposomes bearing a poly(ethylene glycol) derivative with carboxyl groups, Biochim. Biophys. Acta 1193 (1994) 1–9.
[6] K. Kono, T. Igawa, T. Takagishi, Cytoplasmic delivery of calcein mediated by liposomes modified with a pH-sensitive poly(ethylene glycol) derivative, Biochim. Biophys. Acta 1325 (1997) 143–154.
[7] N. Sakaguchi, C. Kojima, A. Harada, K. Kono, Preparation of pH-sensitive poly (glycidol) derivatives with varying hydrophobicities: their ability to sensitize stable liposomes to pH, Bioconjugate Chem. 19 (2008) 1040–1048.
[8] P.A. Bullough, F.M. Hughson, J.J. Skehel, D.C. Wiley, Structure of influenza haemagglutinin at the pH of membrane fusion, Nature 371 (1994) 37–43.
[9] N. Murthy, J.R. Robichaud, D.A. Tirrell, P.S. Stayton, A.S. Hoffman, The design and synthesis of polymers for eukaryotic membrane disruption, J. Controlled Release 61 (1999) 137–143.
[10] C.A. Lackey, N. Murthy, O.W. Press, D.A. Tirrell, A.S. Hoffman, P.S. Stayton, Hemolytic activity of pH-responsive polymer-streptavidin bioconjugates, Bioconjugate Chem. 10 (1999) 401–405.
[11] C.C. Lee, J.A. MacKay, J.M.J. Frechet, F.C. Szoka, Designing dendrimers for biological applications, Nat. Biotechnol. 12 (2005) 1517–1526.
[12] U. Boas, P.M.H. Heegaad, Dendrimers in drug research, Chem. Soc. Rev. 33 (2004) 43–63.
[13] A. Sunder, R. Mulhaupt, R. Haag, H. Frey, Hyperbranched polyether polyols: a modular approach to complex polymer architectures, Adv. Mater. 12 (2000) 235–239.
[14] A. Sunder, J. Heinemann, H. Frey, Controlling the growth of polymer trees: concepts and perspectives for hyperbranched polymers, Chem. Eur. J. 6 (2000) 2499–2506.
[15] H. Frey, R. Haag, Dendritic polyglycerol: a new versatile biocompatible material, Rev. Mol. Biotechnol. 90 (2002) 257–267.
[16] Z. Shen, G. Reznikoff, G. Dranoff, K.L. Rock, Cloned dendritic cells can present exogenous antigens on both MHC class I and class II molecules, J. Immunol. 158 (1997) 2723–2730.
[17] D.L. Daleke, K. Hong, D. Papahadjopoulos, Endocytosis of liposomes by macrophages: binding, acidification and leakage of liposomes monitored by a new fluorescence assay, Biochim. Biophys. Acta 1024 (1990) 352–366.
[18] E. Yuba, C. Kojima, N. Sakaguchi, A. Harada, K. Koiwai, K. Kono, Gene delivery to dendritic cells mediated by complexes of lipoplexes and pH-sensitive fusogenic polymer-modified liposomes, J. Controlled Release 130 (2008) 77–83.
[19] R.D. Hester, P.H. Mitchell, A new universal GPC calibration method, J. Polym. Sci. Chem. Ed. 18 (1980) 1727–1738.

[20] M.A. Yassine, M. Lafleur, C. Meier, H.U. Petereit, J.C. Leroux, Characterization of the membrane-destabilizing properties of different pH-sensitive methacylic acid copolymers, Biochim. Biophys. Acta 1613 (2003) 28–38.
[21] K. Kalyanasundaram, J.K. Thomas, Environmental effects on vibronic band intensities in pyrene monomer fluorescence and their application in studies of micellar systems, J. Am. Chem. Soc. 99 (1977) 2039–2044.
[22] H.G. Schild, D.A. Tirrell, Microheterogeneous solutions of amphiphilic copolymers of N-isopropylacrylamide. An investigation via fluorescence methods, Langmuir 7 (1991) 1319–1324.
[23] K. Tamano, T. Imae, S. Yusa, Y. Shimada, Structure-selective dye uptake into an aggregate of a copolymer with linear polyelectrolyte block and hydrophobic block carrying pendant dendritic moiety in water, J. Phys. Chem. B 109 (2005) 1226–1230.
[24] E. Yuba, C. Kojima, A. Harada, Tana, S. Watarai, K. Kono, pH-Sensitive fusogenic polymer-modified liposomes as a carrier of antigenic proteins for activation of cellular immunity, Biomaterials 31 (2010) 943–951.
[25] D.K. Struck, D. Hoekstra, R.E. Pagano, Use of resonance energy transfer to monitor membrane fusion, Biochemistry 20 (1981) 4093–4099.

Please cite this article as: E. Yuba, et al., Carboxylated hyperbranched poly(glycidol)s for preparation of pH-sensitive liposomes, J. Control. Release (2010), doi:10.1016/j.jconrel.2010.03.001

Cancer Science
The official journal of the Japanese Cancer Association JCA

Mature acinar cells are refractory to carcinoma development by targeted activation of Ras oncogene in adult rats

Hajime Tanaka,[1] Katsumi Fukamachi,[2] Mitsuru Futakuchi,[2] David B. Alexander,[2] Ne Long,[2] Shojiro Tamamushi,[4] Kohtaro Minami,[5] Susumu Seino,[5] Hirotaka Ohara,[1] Takashi Joh[1] and Hiroyuki Tsuda[2,3,6]

[1]Departments of Gastroenterology and Metabolism, [2]Molecular Toxicology and [3]Nanotoxicology Project, Nagoya City University Graduate School of Medical Sciences, Nagoya; [4]CLEA Japan Inc., Shizuoka; [5]Division of Cellular and Molecular Medicine Kobe University Graduate School of Medicine, Kobe, Japan

(Received July 20, 2009/Revised October 8, 2009/Accepted October 13, 2009/Online publication November 16, 2009)

Pancreatic ductal adenocarcinoma (PDA) is one of the most debilitating malignancies in humans. A thorough understanding of the cytogenesis of this disease will aid in establishing successful treatments. We have developed an animal model which uses adult $Hras^{G12V}$ and $Kras^{G12V}$ transgenic rats in which oncogene expression is regulated by the Cre/loxP system and neoplastic lesions are induced by injection of adenovirus-expressing Cre recombinase. When adenovirus with Cre recombinase under the control of the CMV enhancer/chicken β-actin (CAG) promoter (Ad-CAG-Cre) is injected into the pancreatic duct of these animals, pancreatic neoplasias develop. Pathologically, the origin of these lesions is duct, intercalated duct, and centroacinar cells, but not acinar cells. The present study was undertaken to test the effect of acinar cell-specific oncogenic *ras* expression. Adult transgenic rats were injected with adenovirus with Cre recombinase under the control of the acinar cell-specific promoters amylase (Ad-Amy-Cre) and elastase-1 (Ad-Ela-Cre) or under the control of the non-specific CAG promoter. Injection of either Ad-Amy-Cre or Ad-Ela-Cre into the pancreatic ducts of transgenic animals in which oncogenic *Kras* is tagged with hemagglutinin (HA), HA-$Kras^{G12V}$ rats resulted in expression of oncogenic *ras* in acinar cells but not in duct, intercalated duct, or centroacinar cells. Notably, injected animals did not develop any observable proliferative or neoplastic lesions. In marked contrast, injection of Ad-CAG-Cre resulted in pancreatic cancer development within 4 weeks. These results indicate that adult acinar cells are refractory to Ras oncogene activation and do not develop neoplasia in this model. (*Cancer Sci* 2010; 101: 341–346)

Pancreatic ductal adenocarcinoma (PDA) is a highly lethal disease, which is usually diagnosed in an advanced state. Most patients die within 1 year of diagnosis, [1] and the 5-year survival rate is <5%.[2] Understanding of the cytogenesis of PDA offers new directions for targeted therapeutic approaches to combat this disease.

Previously, we reported on an animal model in which pancreatic neoplasia was induced in adult $Hras^{G12V}$ transgenic rats by injection of adenovirus with Cre recombinase under the control of the CMV enhancer/chicken β-actin (CAG) promoter into the pancreatic duct.[3] In these animals, it was shown that duct, intercalated duct, centroacinar, and acinar cells were all infected with the adenovirus, but induced pre-neoplastic and neoplastic lesions were shown to express only duct cell-specific characteristics and not acinar cell-specific characteristics. Moreover, proliferative lesions were not observed in acinar cells. Therefore, we hypothesized that PDA does not develop from adult pancreatic acinar cells in this model.

The present study was undertaken to directly test the capability of mature acinar cells to develop into a neoplastic lesion. Transgenic rats with an Hras or hemagglutinin (HA)-tagged Kras oncogene were injected with Cre recombinase expressing adenoviruses in which Cre expression was under the control of promoters specifically active in acinar cells. Mature acinar cells in injected rats did express active Ras proteins, but did not develop any proliferative or neoplastic lesions.

Materials and Methods

Generation of transgenic rats. For the generation of transgenic rats conditionally expressing human $Kras^{G12V}$ we first made a cDNA fragment encoding the human $Kras4B^{G12V}$ with a 3× HA tag sequence at its 5′ end (HA-$Kras^{G12V}$). The HA-$Kras^{G12V}$ cDNA was subcloned into the SacI/KpnI site of pCALNL5 (DNA Bank, RIKEN Bio Resource Center, Ibaraki, Japan)[4,5] to produce pCALNLHAKras. pCALNLHAKras was digested with SalI/HindIII. The purified cassette (Fig. 1A) was injected into the pronuclei of Sprague–Dawley rats (CLEA Japan, Tokyo, Japan). Techniques used for the generation of transgenic rats were the same as those reported previously.[3,6] A total of 265 injected eggs were transplanted into pseudo-pregnant Sprague–Dawley rats. Of 37 potential transgenic rats screened, four male and one female rat were shown by PCR to carry the transgene. Transgenic founder rats were mated with Sprague–Dawley rats, and offspring were screened for the presence of the transgene by PCR analysis of genomic DNA isolated from tail biopsies at the age of 3 weeks. The following primers were used: 5′-TCTGGATCAAATCCGAACGC-3′, 5′-TGACCTGCTGTGTC-GAGAAT-3′. Two founder rats carrying a CALNLHA$Kras^{G12V}$ transgene transmittable to descendent generations (Kras301and Kras327) and two founder rats (Kras409 and Kras417) carrying a non-tagged $Kras^{G12V}$ transgene were established using the same cassette (data not shown). In this study, we used Kras301 and Kras327. Hras250 rats conditionally expressing human $Hras^{G12V}$ were generated as previously described. [3] They were maintained in plastic cages in an air-conditioned room with a 12-h light/12-h dark cycle. All experiments were conducted according to the Guidelines for Animal Experiments of the Nagoya City University Graduate School of Medical Sciences.

Preparation of adenovirus vectors. Adenoviruses in which either the mouse amylase-2 or the rat elastase-1 promoter drove the expression of Cre recombinase (Ad-Amy-Cre or Ad-Ela-Cre) (Fig. 1B) were prepared as described previously.[7] Recombinant adenovirus vectors carrying the *Cre* gene (Ad-CAG-Cre) (Fig. 1B) and empty adenovirus vector were prepared as described previously.[3] Recombinant adenovirus vectors were amplified in HEK-293 cells and then purified using Vivapure

[6]To whom correspondence should be addressed.
E-mail: htsuda@med.nagoya-cu.ac.jp

doi: 10.1111/j.1349-7006.2009.01410.x

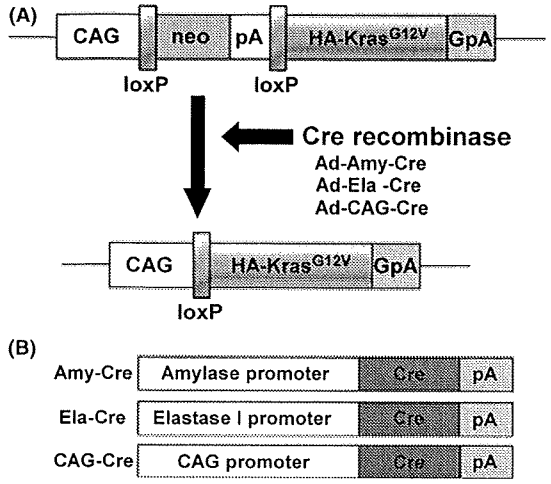

Fig. 1. Conditional expression of Kras^{G12V} transgene. (A) The CALNL-HAKras^{G12V} transgene is comprised of a hybrid CMV enhancer/chicken β-actin (CAG) promoter, a cassette for the neomycin resistance gene flanked by loxP sites, and a sequence containing a human Kras^{G12V} with a hemagglutinin (HA)-tag. Infection with the Cre recombinase-expressing adenovirus results in Cre-mediated recombination of the transgene and removal of the neo-coding region and its associated mRNA polyadenylation signal, generating a functional HA-Kras^{G12V} gene expression unit. GpA, rabbit- β-globin poly(A) site; pA, SV40 early poly(A) site. (B) Cre recombinase with nuclear localization signal expressing adenovirus in which Cre expression is under the control of three different promoters: the amylase promoter and the elastase-1 promoter which are active in acinar cells, and the CAG promoter which is a nonspecific promoter.

Adenopack (Vivascience, Hannover, Germany). The titer of the adenovirus was determined by using the Rapid titer kit (Clontech, Mountain View, CA, USA). The virus stock was concentrated to 1.0×10^{10} pfu/mL.

Induction of active Ras in the pancreas. Adenovirus vectors were injected into the pancreatic ducts of 12-week-old adult male rats through the common duct as previously reported. To induce active Ras specifically in acinar cells, adenoviruses (6×10^8 pfu/rat) in which the expression of Cre recombinase was under the control of acinar cell specific promoters, either the amylase-2 (Ad-Amy-Cre) or elastase-1 (Ad-Ela-Cre) promoter, were used. To induce active Ras non-specifically, adenoviruses (6×10^8 pfu/rat) in which the expression of Cre recombinase was under the control of the non-specific CAG promoter were used.

Western blotting. Western blot analysis and detection of activated Ras protein was performed using a Ras Activation Assay kit (Upstate, Lake Placid, NY, USA) as described previously.[3,8] Concentrations of the proteins were determined by Bio-Rad Protein assay. Proteins were separated by SDS-PAGE. After transfer to a polyviniliden defluoride membrane, the membrane was blocked with 5% nonfat milk and then incubated for 1 h at room temperature with primary antibodies. The following antibodies were used: anti-Ras, clone Ras10 (Upstate) diluted 1:4000; HA-probe (Y-11; Santa Cruz Biotechnology, Santa Cruz, CA, USA) diluted 1:1,000; and monoclonal anti-β-actin (A5441; Sigma, St Louis, MO) diluted 1:10 000. The primary antibodies were detected using HRP-conjugated secondary antibodies (Southern Biotechnology Associates, Birmingham, AL, USA) and ECL plus (GE Heallthcare UK, Buckinghamshire, UK).

Immunostaining. Tissues were fixed in 10% formalin or 4% paraformaldehyde fixative and embedded in paraffin. For Ki67, proliferating cell nuclear antigen (PCNA), and HA-tag staining, sections were boiled for 10 min in a 10-mM citrate buffer (pH 6.0) and then allowed to cool in PBS for 30 min before incubation with antibodies. For anti-α-amylase staining, section slides were incubated for 10 min in a 0.1% trypsin solution at 37°C and then washed in PBS for 5 min before incubation with antibodies.

Before staining, each section was blocked with 10% goat serum (Nichirei Bio Science, Tokyo, Japan) for 5 min at room temperature. The slides were incubated overnight at 4°C with primary antibodies against Ki67antigen (NCL-Ki67-p; Novocastra Laboratories, Newcastle, UK), diluted 1:3000; PCNA (clone PC10; DakoCytomation, Glostrup, Denmark), diluted 1:50; HA-Tag (6E2; Cell Signaling, Danvers, MA, USA), diluted 1:100; or anti-α-amylase (A8273; Sigma, St Louis, MO, USA), diluted 1:200. Slides were incubated with secondary antibodies conjugated with Alexa Fluor488, 546, and 647 (Invitrogen, Carlsbad, CA, USA), and images were obtained with a FLUOVIEW FV300 confocal microscope (Olympus, Tokyo, Japan) or a BZ-9000 fluorescence microscope (Keyence, Osaka, Japan).

Results

Targeted activation of HA-Kras^{G12V} transgenes in mature acinar cells. Injection of transgenic rats with Cre recombinase expressing adenovirus resulted in excision of the stuffer DNA between the CAG promoter and the transgene and consequent expression of the transgene in infected cells (Fig. 1A). Kras301/ 327 rats were injected with Ad-Amy-Cre or Ad-Ela-Cre. Expression of HA-Kras^{G12V} was observed only in amylase-positive acinar cells and not in duct, centroacinar, intercalated duct, or islet cells (Table 2) (Fig. 2A; data for Ad-Ela-Cre is identical to that of Ad-Amy-Cre). Some acinar cells with nuclei with an "owl-eye" or "ground glass" appearance, which are generally used for identification of virus-infected cells,[9] in rats treated with Ad-Amy-Cre or Ela-Cre were also positive for both amylase and HA (Fig. 2A-d,e). All acinar cells positive for HA were entirely negative for Ki67 (Fig. 2A).

Lack of PDA development by targeted activation of Ras^{G12V} in mature acinar cells. None of the Kras301/327 rats injected with Ad-Amy-Cre or Ela-Cre developed pancreatic lesions (Ad-Amy-Cre, 0 out of 5; Ad-Ela-Cre, 0 out of 7) after 8 weeks (Fig. 2B, Table 1). Similarly, none of the Hras250 rats injected with Ad-Amy-Cre or Ad-Ela-Cre (6×10^8 pfu/rat) developed pancreatic lesions (Ad-Amy-Cre, 0 out of 7; Ad-Ela-Cre, 0 out of 8) after 8 weeks (Table 1). In addition, Kras301/327 rats injected with higher titers of Ad-Amy-Cre (6×10^9 pfu/rat) did not develop pancreatic lesions (data not shown). Finally, tumor induction was not observed in injected Kras301/327 rats even after 6 months (data not shown).

Neoplasia development by activation of Ras^{G12V} transgenes in ductular cells. Both Kras301/327 and Hras250 rats injected with Ad-CAG-Cre (6×10^8 pfu/rat) developed pancreatic neoplasias: 22 of 22 Kras301/327 rats and 30 of 35 and Hras250 rats after 2 to 4 weeks (Table 1), as observed in our previous report.[3] Pancreatic neoplasias were also observed in Kras301/327 rats injected with lower titers of Ad-CAG-Cre (6×10^7 pfu/rat) (data not shown). Activation of the transgene in the pancreatic ductal lesions of Kras301/327 rats was shown by Western blotting using anti-HA antibody (Fig. 3). The expression of HA-Kras^{G12V} was detected in pancreatic intraepithelial neoplasia (PanIN) and neoplastic lesions, but not in normal-looking pancreatic duct cells or stromal cells (Fig. 4A). Ki67 or PCNA and HA were positive in PanIN lesions (Fig. 4B) and in many neoplastic cells (Fig. 4C).

Discussion

The morphological and molecular signatures associated with human pancreas tumors suggests that duct epithelium is

doi: 10.1111/j.1349-7006.2009.01410.x

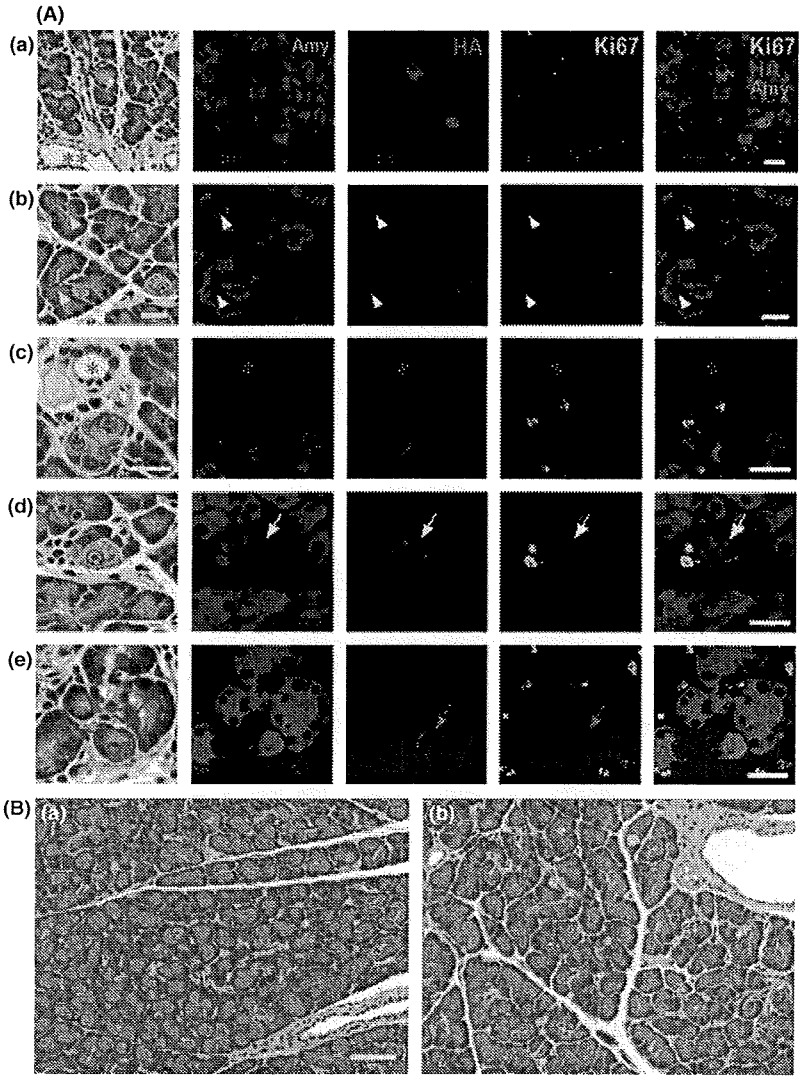

Fig. 2. Acinar cell-specific expression of hemagglutinin (HA)-Kras^{G12V}. (A) Localization of amylase (blue) protein, HA-Kras^{G12V} (red) and Ki67 (green) at 2 days after injection of virus with Ad-Amy-Cre (a, b, c, d) and Ela-Cre (e). All the HA-Kras^{G12V} positive cells (red) were acinar cells; expression was not observed in duct cells (**), centroacinar cells (yellow arrowhead), or small duct cells (*). Most virally infected acinar cells positive for HA-Kras^{G12V} were indistinguishable from non-infected acinar cells by hematoxylin–eosin staining. Some infected acinar cells have nuclei with a so-called "owl-eye" (yellow arrows) or "ground glass" (red arrows) appearance. Ki67 (green) is not present in the nuclei of the cells expressing HA-Kras^{G12V} (red). Bar, 20 μm. (B) None of the Ad-Amy-Cre (a) or the Ad-Ela-Cre (b) groups displayed any pancreatic lesions, even after 8 weeks. Bar, 50 μm.

responsible for the development of PDA, but it remains unclear whether other pancreatic cells might also contribute to the cytogenesis of these lesions. In our previous study using the Hras250 rat, 4 weeks after injection of adenovirus with Cre recombinase under the control of the constitutive CAG promoter, proliferative lesions in the duct epithelium, intercalated ducts, and centroacinar cells were widespread, but we could not detect any proliferative lesions in acinar cells; moreover, subsequent neoplastic lesions expressed only duct cell-specific characteristics and not acinar cell-specific ones.[3] We have obtained essentially identical results with Kras transgenic rats as we did with Hras250 rats (data not shown). These results suggest that PDAs may arise from centroacinar cells, intercalated duct, or pancreatic duct epithelium, but not from acinar cells.

The current study was undertaken to clarify whether mature acinar cells in adult rats could be induced to develop to PDA by targeted activation of oncogenic *ras*. Activation of oncogenic *ras* in acinar cells did not lead to the development of any observable pancreatic lesions, while nonspecific activation of oncogenic *ras* in the pancreas resulted in rapid development of

Table 1. Pancreas tumor induction by activation of Hras^{G12V} or hemagglutinin (HA)-Kras^{G12V} oncogene after Cre-adenovirus injection

Oncogene	Virus vector	Number of rats with tumor (%)
Hras^{G12V}	Amylase-Cre	0/7 (0)
	Elastase-Cre	0/8 (0)
	CAG-Cre	30/35 (87.5)
HA-Kras^{G12V}	Amylase-Cre	0/5 (0)
	Elastase-Cre	0/7 (0)
	CAG-Cre	22/22 (100)

Table 2. Target cell and tumor type in Hras^{G12V} and hemagglutinin (HA)-Kras^{G12V}transgenic rats

Virus vector	Target cells			Tumor yield	
	Acinar cells	Centroacinar cells	Duct cells	Acinar cells	Duct cells
Amy-Cre	+	–	–	–	–
Ela-Cre	+	–	–	–	–
CAG-Cre[3]	+	+	+	–	+

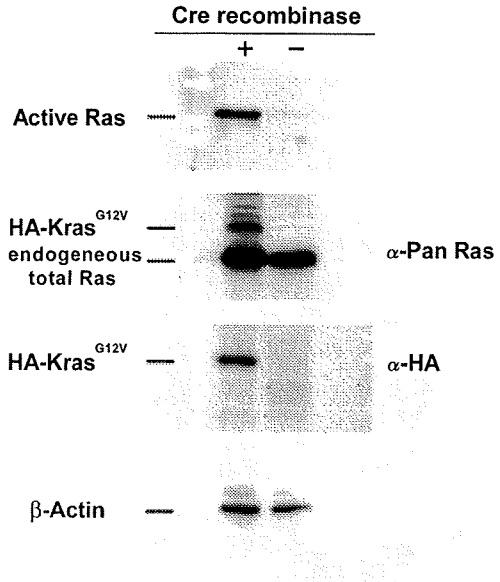

Fig. 3. Transgene activation in Kras301 and 327 by Western blotting. A high level of active Ras and hemagglutinin (HA)-Kras^{G12V} were detected in the pancreas of the Ad-CAG-Cre-treated rats. The amount of active Ras was analyzed by RBD (Ras-binding domain of Raf-1) pull-down assay followed by Western blotting with anti-pan Ras antibody. HA-Kras^{G12V} and endogeneous total Ras was detected using anti-Pan Ras antibody. HA-Kras^{G12V} was detected using anti-HA antibody. β-Actin was used as a loading control.

pancreatic neoplasias. Our results clearly show that conditional expression of oncogenic *ras* in acinar cells in fully developed pancreas tissue does not result in induction of neoplasia in this model (Table 1).

Previous reports in which Kras was activated in immature acinar cells during embryonic development[10,11] suggested that acinar-ductal metaplasia played a role in the development of PDA. In these models, premalignant acinar-ductal metaplasia and acinar tumor mixed with duct-like lesions developed in transgenic mice. This acinar-ductal metaplasia, however, may have occurred before the pancreas fully developed. Our model, on the other hand, targets mature acinar cells which express digestive enzymes, amylase and/or elastase, and these cells do not undergo acinar-ductal metaplasia in response to ras activation.

Our results are in agreement with a recent study in which the distribution of *K-RAS2* gene mutations was extensively examined in surgically resected pancreata from human patients and which concluded that ductal neoplasms of the human pancreas did not appear to arise from acinar cells.[12]

Kras mutations were not observed in pancreatic acinar cell carcinoma (ACC) induced in mature rats by administration of azaserine.[13] Furthermore, alterations in the APC/β-catenin pathway were detected in 23.5% of human ACC,[14] but mutation of Kras was not observed.[15,16] Thus, it is possible that APC/β-catenin or another pathway, but not necessarily Kras activation, is involved in ACC development.

While pancreas cancer in the hamster model is also believed to arise from ductal epithelial hyperplasia,[17,18] several studies using transgenic mice[11,19–24] suggest that PDA may develop from acinar cells. In most of these studies, however, oncogenic stimuli are present during embryonic development, prior to the development of a mature pancreas. Therefore, the acinar cells which were activated and developed into neoplasias in these models could very well be at a different developmental stage to the acinar cells which are present in a mature pancreas. This is important because the majority of PDA patients are 60 years of age or older. It is highly unlikely that an oncogenic insult occurring in the uterus is the root cause of most of these PDAs. Moreover, epidemiological studies indicate the incidence of PDA is closely related to lifestyle.[25] Therefore, PDA most likely develops from cells in the mature pancreas. Consequently, pancreas tumor models in which the oncogenic insult occurs during embryonic development are unlikely to be appropriate for determining the cytogenesis of human PDA.

Two models[22–24] use conditional activation of Cre recombinase to active oncogenic *ras* in adult animals: one model[22] uses the tet-off system to control expression of Cre recombinase and the other model[23,24] uses the tamoxifen-estrogen receptor system to control nuclear localization of Cre recombinase. These studies had slightly conflicting results. In one study, expression of oncogenic *ras* in adult acinar cells did not by itself induce pancreatic lesions; additional treatment causing chronic pancreatitis was also needed.[22] In the other study, expression of oncogenic *ras* was sufficient to induce PanIN-like lesions.[23,24] In our model, we clearly showed that while expression of oncogenic *ras* is sufficient to induce duct, intercalated duct, and/or centroacinar cells to develop into pancreatic cancers, it is not sufficient to induce acinar cells to develop into pancreatic cancers. Whether these discrepancies are due to experimental procedures, the nature of the Cre recombinase constructs used, or differences between mice and rats remains to be resolved. There are however, a few readily apparent differences. In our rat system, there is no expression of Cre recombinase in the animal until injection of adenovirus-expressing Cre recombinase, and the expression of Cre recombinase is transient. In the model which uses tamoxifen, on the other hand, Cre recombinase is expressed during embryonic development, but nuclear localization is regulated by tamoxifen.[23,24] In this model, however, there was a low level of tamoxifen-independent recombination events resulting in expression of oncogenic *ras* in embryonic acinar cells.[24] It is possible that embryonic acinar cells expressing oncogenic *ras* did not fully differentiate in the adult pancreas; for example, in the mouse colon expression of Kras^{G12V} inhibits differentiation.[26] Therefore, it is possible that in the tamoxifen-estrogen regulated model,[23,24] the acinar cells which were activated to undergo metaplasia to duct-like cells in the adult were not actually mature acinar cells. The other obvious difference is that in the model regulated by the tet-off system, two events were required to induce pancreas cancer: activation of oncogenic *Kras* and chronic pancreatitis.[22] Chronic pancreatitis would very likely result in the death of mature acinar cells and their replacement from a proliferative compartment. It is possible that these replacement cells are not fully mature acinar cells, again suggesting the possibility that the acinar cells which underwent metaplasia to duct-like cells were not actually mature acinar cells.

The primary aim of this study was to determine whether activation of oncogenic Kras in mature, digestive enzyme-secreting acinar cells would lead to pancreatic lesions. Our findings support our earlier hypothesis that PDA does not develop from Kras activation in mature acinar cells. It is possible, however, that PDA could develop from Kras activation in immature acinar cells, and in this regard we would like to emphasize the results of Guerra *et al.*[22] in which activation of Kras in the mature pancreas accompanied by chronic pancreatitis resulted in induction of PDA in transgenic mice. Importantly, chronic pancreatitis has been shown to be one of the main risk factors for PDA development in humans.[27,28]

Other factors which may influence PDA development in our model are inflammation and fibrosis. Shortly after infection of pancreatic tissue with Cre recombinase carrying adenovirus to activate the Kras transgene, infiltration of macrophages and lymphocytes could be observed. This infiltration is presumably in response to viral infection. A moderate degree of inflammation, however, was still observed in the stromal tissue surrounding the tumors when PDA developed. These finding suggest that

doi: 10.1111/j.1349-7006.2009.01410.x

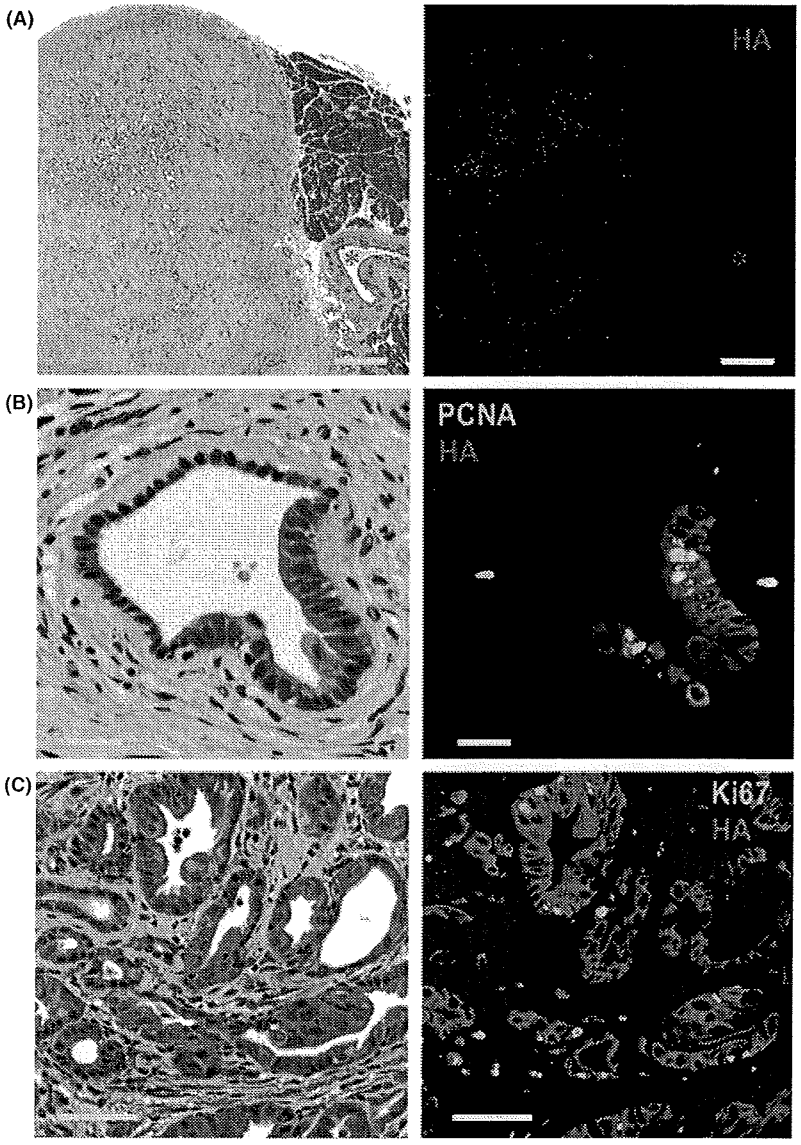

Fig. 4. Pancreatic ductal adenocarcinoma (PDA) induced by injection of Ad-CAG-Cre in Kras301/327 rats. (A) The expression of hemagglutinin (HA)-$Kras^{G12V}$ (red) was seen only in PDA lesions (on the left of photo), and not in stromal cells, acinar cells (on the right of photo), or normal pancreatic duct cells (*). Bar, 500 μm. (B) A pancreatic intraepithelial neoplasia (PanIN) lesion was surrounded by fibrous tissue with some infiltration of inflammatory cells. Expression of proliferating cell nuclear antigen (PCNA) (green) and HA protein (red) in a PanIN lesion in rats of the CAG-Cre group. PCNA is preferentially expressed in PanIN cells. Bar, 20 μm. (C) Expression of Ki67 (green) and HA protein (red) in PDA cells. Many PDA cells (red) are simultaneously positive for Ki67. Bar, 50 μm.

inflammation may play a role in PDA development in this model. However, interaction between the immune system and tumors is complex and whether inflammation actually promotes PDA development in this model remains to be examined.

A current study has demonstrated that the fibrous element accompanying inflammation can also play an important role in cancer development.[29] This aspect of PDA development in our model also remains to be examined.

In summary, while there are discrepancies between different animal models of pancreatic cancer, our results indicate that expression of oncogenic *ras* in fully mature acinar cells does not induce cell proliferation or result in development of any pancreatic lesions. Thus, we conclude that mature acinar cells are not the origin of PanIN or pancreatic neoplasia in this model.

Acknowledgments

We thank Dr T. Shirai (Nagoya City University) for his kind advice for histological examination and assistance in histological specimen preparation. This work was supported in part by a Grant-in-Aid for Scientific Research (C) from Japan Society for the Promotion of Science; a Grant-in-Aid for Cancer Research (15-2, 16-13, 17S-6, 20S-8) from the Ministry of Health, Labour and Welfare, Japan; a Grant-in-Aid for Research on Nanotechnical Medical (H19-Nano-Ippan-014) from the Ministry of Health, Labour, and Welfare of Japan; a Grant-in-Aid for Research on Risk of Chemical Substances (H19-Kagaku-Ippan-006) from the Ministry of Health, Labour, and Welfare of Japan; and a Grant-in-Aid for Nagoya Ohjinkai Young Investigators Medical Research Award from Nagoya City University, Japan.

References

1 Beger HG, Rau B, Gansauge F, Poch B, Link KH. Treatment of pancreatic cancer: challenge of the facts. *World J Surg* 2003; **27**: 1075–84.
2 Jemal A, Siegel R, Ward E, Murray T, Xu J, Thun MJ. Cancer statistics, 2007. *CA Cancer J Clin* 2007; **57**: 43–66.
3 Ueda S, Fukamachi K, Matsuoka Y *et al.* Ductal origin of pancreatic adenocarcinomas induced by conditional activation of a human Ha-ras oncogene in rat pancreas. *Carcinogenesis* 2006; **27**: 2497–510.
4 Kanegae Y, Lee G, Sato Y *et al.* Efficient gene activation in mammalian cells by using recombinant adenovirus expressing site-specific Cre recombinase. *Nucleic Acids Res* 1995; **23**: 3816–21.

5 Niwa H, Yamamura K, Miyazaki J. Efficient selection for high-expression transfectants with a novel eukaryotic vector. *Gene* 1991; **108**: 193–9.
6 Asamoto M, Ochiya T, Toriyama-Baba H *et al.* Transgenic rats carrying human c-Ha-ras proto-oncogenes are highly susceptible to N-methyl-N-nitrosourea mammary carcinogenesis. *Carcinogenesis* 2000; **21**: 243–9.
7 Minami K, Okuno M, Miyawaki K *et al.* Lineage tracing and characterization of insulin-secreting cells generated from adult pancreatic acinar cells. *Proc Natl Acad Sci U S A* 2005; **102**: 15116–21.
8 Fukamachi K, Imada T, Ohshima Y, Xu J, Tsuda H. Purple corn color suppresses Ras protein level and inhibits 7,12-dimethylbenz[a]anthracene-induced mammary carcinogenesis in the rat. *Cancer Sci* 2008; **99**: 1841–6.
9 Kobayashi TK, Sato S, Tsubota K, Takamura E. Cytological evaluation of adenoviral follicular conjunctivitis by cytobrush. *Ophthalmologica* 1991; **202**: 156–60.
10 Schmid RM. Acinar-to-ductal metaplasia in pancreatic cancer development. *J Clin Invest* 2002; **109**: 1403–4.
11 Grippo PJ, Nowlin PS, Demeure MJ, Longnecker DS, Sandgren EP. Preinvasive pancreatic neoplasia of ductal phenotype induced by acinar cell targeting of mutant Kras in transgenic mice. *Cancer Res* 2003; **63**: 2016–9.
12 Shi C, Hong SM, Lim P *et al.* KRAS2 mutations in human pancreatic acinar-ductal metaplastic lesions are limited to those with PanIN: implications for the human pancreatic cancer cell of origin. *Mol Cancer Res* 2009; **7**: 230–6.
13 Longnecker DS, Curphey TJ. Adenocarcinoma of the pancreas in azaserine-treated rats. *Cancer Res* 1975; **35**: 2249–58.
14 Abraham SC, Wu TT, Hruban RH *et al.* Genetic and immunohistochemical analysis of pancreatic acinar cell carcinoma: frequent allelic loss on chromosome 11p and alterations in the APC/beta-catenin pathway. *Am J Pathol* 2002; **160**: 953–62.
15 Terhune PG, Memoli VA, Longnecker DS. Evaluation of p53 mutation in pancreatic acinar cell carcinomas of humans and transgenic mice. *Pancreas* 1998; **16**: 6–12.
16 Van Kranen HJ, Vermeulen E, Schoren L *et al.* Activation of c-K-ras is frequent in pancreatic carcinomas of Syrian hamsters, but is absent in pancreatic tumors of rats. *Carcinogenesis* 1991; **12**: 1477–82.
17 Tsutsumi M, Kondoh S, Noguchi O *et al.* K-ras gene mutation in early ductal lesions induced in a rapid production model for pancreatic carcinomas in Syrian hamsters. *Jpn J Cancer Res* 1993; **84**: 1101–5.
18 Tsutsumi M, Konishi Y. Precancerous conditions for pancreatic cancer. *J Hepatobiliary Pancreat Surg* 2000; **7**: 575–9.
19 Tuveson DA, Zhu L, Gopinathan A *et al.* Mist1-KrasG12D knock-in mice develop mixed differentiation metastatic exocrine pancreatic carcinoma and hepatocellular carcinoma. *Cancer Res* 2006; **66**: 242–7.
20 Hingorani SR, Petricoin EF, Maitra A *et al.* Preinvasive and invasive ductal pancreatic cancer and its early detection in the mouse. *Cancer Cell* 2003; **4**: 437–50.
21 Wagner M, Luhrs H, Kloppel G, Adler G, Schmid RM. Malignant transformation of duct-like cells originating from acini in transforming growth factor transgenic mice. *Gastroenterology* 1998; **115**: 1254–62.
22 Guerra C, Schuhmacher AJ, Canamero M *et al.* Chronic pancreatitis is essential for induction of pancreatic ductal adenocarcinoma by K-Ras oncogenes in adult mice. *Cancer Cell* 2007; **11**: 291–302.
23 Habbe N, Shi G, Meguid RA *et al.* Spontaneous induction of murine pancreatic intraepithelial neoplasia (mPanIN) by acinar cell targeting of oncogenic Kras in adult mice. *Proc Natl Acad Sci U S A* 2008; **105**: 18913–8.
24 De La OJ, Emerson LL, Goodman JL *et al.* Notch and Kras reprogram pancreatic acinar cells to ductal intraepithelial neoplasia. *Proc Natl Acad Sci U S A* 2008; **105**: 18907–12.
25 Jiao L, Mitrou PN, Reedy J *et al.* A combined healthy lifestyle score and risk of pancreatic cancer in a large cohort study. *Arch Intern Med* 2009; **169**: 764–70.
26 Haigis KM, Kendall KR, Wang Y *et al.* Differential effects of oncogenic K-Ras and N-Ras on proliferation, differentiation and tumor progression in the colon. *Nat Genet* 2008; **40**: 600–8.
27 Lowenfels AB, Maisonneuve P, Cavallini G *et al.* Pancreatitis and the risk of pancreatic cancer. International Pancreatitis Study Group. *N Engl J Med* 1993; **328**: 1433–7.
28 Malka D, Hammel P, Maire F *et al.* Risk of pancreatic adenocarcinoma in chronic pancreatitis. *Gut* 2002; **51**: 849–52.
29 Sangai T, Ishii G, Kodama K *et al.* Effect of differences in cancer cells and tumor growth sites on recruiting bone marrow-derived endothelial cells and myofibroblasts in cancer-induced stroma. *Int J Cancer* 2005; **115**: 885–92.

doi: 10.1111/j.1349-7006.2009.01410.x